A Review of Flexible Bronchoscope Robots for Peripheral Pulmonary Nodule Intervention

Yuzhou Duan, *Student Member, IEEE*, Jie Ling, *Member, IEEE*, Micky Rakotondrabe, *Member, IEEE*, Zuoqing Yu, Lei Zhang, and Yuchuan Zhu, *Member, IEEE*

***Abstract*—The development of procedure-specific surgical robots has become essential for tackling complex clinical challenges. Flexible bronchoscope robots (FBRs) have emerged over the past decade, revealing broad prospects for the safe, precise, and reliable diagnosis of peripheral pulmonary nodules (PPNs), which is crucial for enabling early lung cancer treatment. However, in advancing FBR development, roboticists sometimes stray from or overlook practical surgical considerations, which might impede its clinical implementation. This review aims to bridge this gap by offering an engineering-focused perspective enriched with critical medical insights to drive the clinical translation of next-generation FBRs. We begin by highlighting the medical significance and current state of FBR research. Then, we outline the "ambient environments" of FBRs: the supported procedure, robotic system, steering tools, and deployment modes. Subsequently, we summarize recent progress in FBR technology, focusing on two key areas: procedure-specific design and modeling to improve intervention capabilities, and autonomous navigation and control strategies to enhance autonomy. Based on the given analysis, we discuss the development directions of next-generation FBRs according to the current clinical challenges and the engineering approaches to their realization.**

***Index Terms*—Continuum robot, minimally invasive surgery, peripheral pulmonary nodule biopsy, robotic-assisted bronchoscopy, surgical robot.**

I. Introduction

CONTINUUM robots have found a suitable place in minimally invasive surgery (MIS) for their slenderness and flexibility. Since MIS is moving decidedly toward minimizing the size and number of visible skin incisions while maintaining the intervention precision [1], advanced studies are focusing on developing delicate continuum robots that offer enhanced maneuverability, multifunctionality, and reduced invasiveness [2], [3]. Especially, this evolution is greatly accelerated in some cutting-edge MIS with strong clinical requirements [4].

In this review, we summarize the engineering advancements related to a new type of continuum robot, known as *flexible bronchoscope robot (FBR)*. The FBR is designed to enhance a cutting-edge MIS procedure—the diagnosis and treatment of peripheral pulmonary nodules (PPN) through flexible bronchoscopy—thereby aiming to improve the survival rates for lung cancer patients [5], [6], [7]. The relevant surgical procedure is referred to as *robot-assisted bronchoscopy (RAB)*.

In the remainder of this section, we first introduce the clinical background of the FBR to highlight its significance. Next, we briefly describe the research status of both commercial products and laboratory studies on FBRs. Finally, we state the motivations, contributions, and organizations of this review.

A. Clinical Background

Lung cancer is the leading cause of cancer-related deaths worldwide [8]. The American Cancer Society reports that approximately 340 people die from lung cancer each day in 2024, nearly 2.5 times more than the next most common cancer (colorectal cancer) [9]. The benefits of improving five-year survival rates by early diagnosis and treatment of lung cancer are self-evident. However, due to the lack of clinical symptoms with early-stage lung cancer, the vast majority of clinically diagnosed lung cancer cases are already advanced. In the past two decades, mainly due to the sustainable development and promotion of lung cancer screening procedures [10], there has been an increasing detection of small ($\leq$10 mm) and even micro ($\leq$5 mm) pulmonary nodules. Furthermore, around 70% of the recently detected cancerous nodules are located in the periphery of the lungs, and this ratio can grow to 80% when considering the lung screening program [11].

Generally, biopsy procedures are necessary to diagnose cancer, and help determine prognosis and plan treatment. However, current first-line surgical procedures, including transbronchial biopsy (TBB) and transthoracic biopsy (TTB), do not respond well to the increasing number of detected PPNs. For the TBB procedure, endobronchial ultrasound with transbronchial needle aspiration (EBUS-TBNA) is a very safe and effective biopsy procedure with high biopsy rates

Received 23 January 2025; revised 29 April 2025; accepted 15 June 2025. Date of publication 25 June 2025; date of current version 21 August 2025. This article was recommended for publication by Associate Editor R. Muradore and Editor P. Dario upon evaluation of the reviewers' comments. This work was supported in part by the Natural Science Foundation of Jiangsu Province under Grant BK20210294; in part by the International Joint Laboratory of Sustainable Manufacturing, Ministry of Education and the Fundamental Research Funds for the Central Universities under Grant NG2024016; in part by the Outstanding Doctoral Dissertation in NUAA under Grant BCXJ25-10; and in part by the Postgraduate Research and Practice Innovation Program of Jiangsu Province under Grant KYCX24_0556. *(Corresponding authors: Jie Ling; Yuchuan Zhu.)*

Yuzhou Duan, Jie Ling, Zuoqing Yu, and Yuchuan Zhu are with the College of Mechanical and Electrical Engineering, Nanjing University of Aeronautics and Astronautics, Nanjing 210016, China (e-mail: dyz@nuaa.edu.cn; meejling@nuaa.edu.cn; meezqyu@nuaa.edu.cn; meeyczhu@nuaa.edu.cn).

Micky Rakotondrabe is with the University of Technologie Tarbes Occitanie Pyrénées, University of Toulouse alliance, 65016 Tarbes, France (e-mail: mrakoton@uttop.fr).

Lei Zhang is with the Department of Respiratory and Critical Care Medicine, NHC Key Laboratory of Respiratory Diseases, Tongji Hospital, Tongji Medical College, Huazhong University of Science and Technology, Wuhan 430030, China (e-mail: 332994261@qq.com).

Digital Object Identifier 10.1109/TMRB.2025.3583172

(≈80%) in patients with centrally located nodules [12], [13]. Nevertheless, due to the tortuosity, narrowness, and multi-branch characteristics of bronchus anatomy in the peripheral lung, its utility for PPNs is limited [14]. For the TTB procedure, although this procedure performs well in diagnosis rates for PPNs (e.g., image-guided transthoracic core needle biopsy with biopsy rates of ≈90% [15]), this procedure has a higher probability of complications (≈43% [16]). In the context of the large number of pulmonary nodules currently being detected and only 5% of pulmonary nodules being cancerous [17], the risks and benefits of this technique are not acceptable.

In this context, FBRs have been developed to overcome the current predicaments in PPN biopsies. By combining human cognitive skills with the precision and robustness of robotic systems, FBRs enable easier access to peripheral lung regions, enhancing biopsy accuracy while ensuring safety.

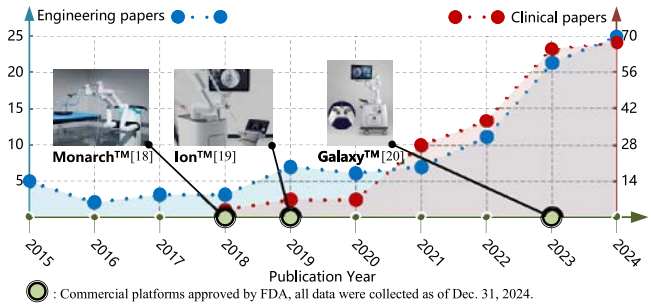

Fig. 1. The chart depicts the annual publication trends of journal and conference papers on flexible bronchoscope robots (FBRs) from 2015 to 2024, categorized into engineering (blue curve) and clinical (red curve) domains. The green dots along the timeline mark the years when commercial platforms received the Food and Drug Administration (FDA) approval. Images of commercial FBRs are reproduced from [18], [19], [20].

B. Research Status

Although continuum robots and flexible bronchoscopes both emerged around six decades ago [21], [22], the concept of FBRs was not introduced until the past decade, with the first prototype study proposed by the Webster III and Alterovitz's teams [23]. To contextualize the background of FBRs, a brief historical review of continuum robots is provided below.

Continuum robotics began to dvelop rapidly in the 1990s and gained further momentum in the early 2000s, with designs often inspired by biological structures such as snakes, trunks, and tentacles. For instance, Choset et al. pioneered the development of snake-like robots for navigating confined and tortuous environments [24], [25]. Around the same time, Webster III and Dupont's teams introduced concentric tube robots. Subsequently, Webster III's team advanced key theoretical frameworks for continuum robot modeling, including piecewise constant curvature models and actuation principles [26], [27], [28]. These foundational studies collectively laid the groundwork for applying continuum robots in MIS and paved the way for the development of FBRs. In recent years, a growing number of continuum robots with diverse designs and increasingly sophisticated modeling and control strategies have been developed; for detailed reviews, see [29], [30], [31], [32], [33].

These abovementioned progress in continuum robotics, coupled with clinical needs, have propelled FBR's momentum during its first decade. As presented in Fig. 1, RAB has attracted considerable interest from both the academic and commercial robotics communities. More than twenty research groups, including bronchoscopists and roboticists, have made efforts on this topic. The number of papers on FBR has rapidly grown from only 5 in 2015 to approximately 300 in total by the end of 2024. Three commercial products (Auris Health's Monarch platform, Intuitive Surgical's Ion System, and Noah Medical's Galaxy System) have been developed and approved by the Food and Drug Administration (FDA). Clinical papers typically focus on topics such as the evaluation, application, and comparative analysis of commercial RAB systems, whereas engineering papers are generally centered on the development of more advanced FBRs. In short, RAB has evolved into a rapidly developing research area, characterized by its distinct procedure-specific design.

Commercial RAB platforms have undergone a series of clinical trials after receiving FDA approval, and the latest studies confirm the effectiveness of RAB. Multiple meta-analyses of RAB suggest that the diagnosis rate of PPNs is about 80-85%, and the complication probability is similar to that of conventional bronchoscopy [34], [35], [36]. In addition, RAB demonstrates enhanced robustness in diagnosing PPNs, even in cases where these nodules exhibit challenging characteristics such as small size [37], no bronchus sign [34], tortuous approach path [38], and eccentric radial-EBUS (rEBUS) view [39]. Furthermore, some studies have been conducted on combining the diagnosis and treatment to streamline the surgical procedure, thereby alleviating hospital workload and avoiding further progression of the cancerous nodule [40], [41]. Last, studies of RAB integrated with other medical images such as computed tomography (CT) and fluoroscopy have been preliminarily carried out [42], [43]. Aided by the accuracy of the RAB and the additional vision of medical modalities, the location of the PPN can be reconfirmed to ensure the correct position of the invasive tools.

Researchers, however, generally think beyond immediate commercial development, looking toward future innovations of FBR. Progress can be divided into two key areas. First, the patient-specific designs, which incorporate advancements in soft and continuum robotics, aim to create systems more attuned to the unique challenges of the pulmonary environment. Second, enhancing FBR autonomy through advanced navigation and control strategies. These advancements aim to surpass the bronchoscopists' traditional sensorimotor capabilities, thereby further enhancing the ability to intervene in PPNs.

C. Motivations and Contributions

1) Motivations: Over the past five years, numerous clinical reviews have been published discussing the current commercial products and their clinical trials, addressing aspects such as system functions [45], [46], clinical performance [47], [48], and technology integration [49]. However, despite the emergence of many new FBRs and advancements in related navigation and control technologies, to the best of the authors'

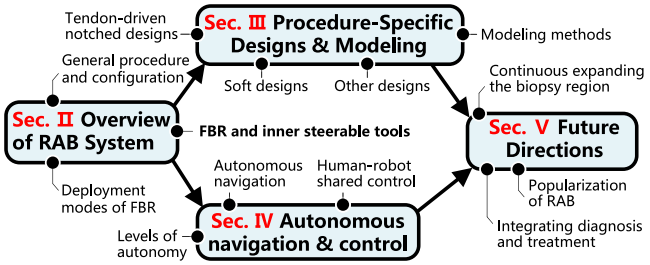

Fig. 2. The main content and organization of this review. Arrows represent logical relationships among sections. Parts indicated by "•—" represent the subsections. Abbreviations: FBR, flexible bronchoscope robot; RAB: robotic-assisted bronchoscopy.

knowledge, no engineering-focused review has yet been published that offers a comprehensive summary of these newly proposed FBRs. Additionally, while recently developed FBRs showcase innovative features, the specific clinical problems they aim to address remain somewhat unclear, which may impede the successful clinical translation of these robots.

2) Contributions: This review adopts an engineering perspective while integrating relevant medical insights, aiming to clarify the latest progress in FBRs and the related clinical challenges. It seeks to guide roboticists in developing the next generation of FBRs that meet pressing clinical needs amidst the rapid evolution of continuum robotics. The main content and structure of this review is presented in Fig. 2, and the key contributions of this review are summarized as follows:

- Proposing an engineering-focused overview of FBR's decade-long development for the first time.
- Providing a detailed summary of the medical background pertinent to RAB, to assist roboticists in understanding the specific clinical contexts essential for the advancement of FBR technology. (Section II)
- Organizing and categorizing procedure-specific designs of FBRs to highlight how the specific features contribute to improving biopsy capabilities, as well as to discuss the remaining challenges. (Section III)
- Dividing the FBR's levels of autonomy (LOAs) to refine the research roadmap and summarizing the latest advancements in terms of autonomous navigation and human-robot shared control. (Section IV)
- Proposing three development directions for the next-generation FBRs based on clinical demands, and discussing the potential engineering approaches for the realization. (Section V)

II. Overview of Robotic-Assisted Bronchoscopy System

Clearly defining the role of FBR in the RAB is crucial for clinical translation. This section provides a brief overview of the RAB to assist roboticists in making more comprehensive considerations when developing advanced FBRs (Fig. 3). We first introduce the procedure and configuration of the RAB system. Then, the FBR and advanced inner tools, typically steerable guide sheathes (GSs) and needles, are clearly defined. Last, we classify three modes for FBR deployment to help roboticists develop FBR while aligning with clinical practices.

A. General Procedure and Configuration

1) General Procedure: The RAB system is not without foundation; it has evolved from conventional navigation and interventional bronchoscopy techniques [14], [50]. As shown in Fig. 3(a), the general procedure of RAB is briefly outlined for easy understanding of roboticists. More detailed clinical descriptions can be found in [45], [51], [52]. The procedure begins with preoperative thin-slice CT scanning to map the pulmonary segmental anatomy. The resulting CT data is then transferred to specialized software (e.g., PlanPoint) for motion planning. This process involves extracting a three-dimensional (3-D) model of the tracheobronchial tree, marking the target lesion, and automatically generating accessible paths. Bronchoscopists can modify these paths based on clinical judgment.

Intraoperatively, the patient is placed in a supine position under general anesthesia to minimize bronchus movement and stabilize the navigation environment. Following airway inspection, the FBR is registered based on a built-in micro-camera and other sensors such as the fiber-optic sensor (FOS) or electromagnetic sensor (EMS) to synchronize its position with the preoperative map. Then, the navigation is enabled. The real-time position of the FBR is tracked by the aforementioned sensors and displayed on a human-robot interface (HRI), guiding the bronchoscopist in delivering the FBR to the PPN with confidence.

One significant challenge in navigation is the CT-to-body divergence, i.e., the discrepancy between the preoperative CT and the patient's anatomy during surgery, mainly caused by differences in breathing patterns and intraoperative tissue deformation. To address this, confirmation using additional intraoperative imaging modalities such as rEBUS, cone beam CT (CBCT), or augmented fluoroscopy is often necessary to accurately localize the lesion or verify "tool-in-lesion" placement. After confirmation, multiple biopsies are taken using tools such as fine needles, brushes, forceps, or advanced techniques like cryobiopsy [53]. Rapid on-site cytological evaluation (ROSE) may be conducted to rapidly examine the biopsy results [54]. In advanced RAB concepts, the clinical outcomes obtained can be rapidly applied to treatment planning. For early-stage cancerous PPN, advanced in situ treatment via FBR may be considered, such as microwave ablation, radiofrequency ablation, and cryoablation [55], [56], [57].

2) System Configuration: RAB systems typically operate on a telerobotic paradigm, involving human-in-the-loop teleoperation of robot-actuated tools [58]. As shown in Fig. 3(b), the system consists of a controller (leader device), a FBR (follower robot) mounted on a robotic platform, and a communication network connecting the two. The controller, often a simple gamepad, is used because typically only a single manipulation arm is involved [44], [59]. The bronchoscopists operate the follower robots remotely from the patient's side.

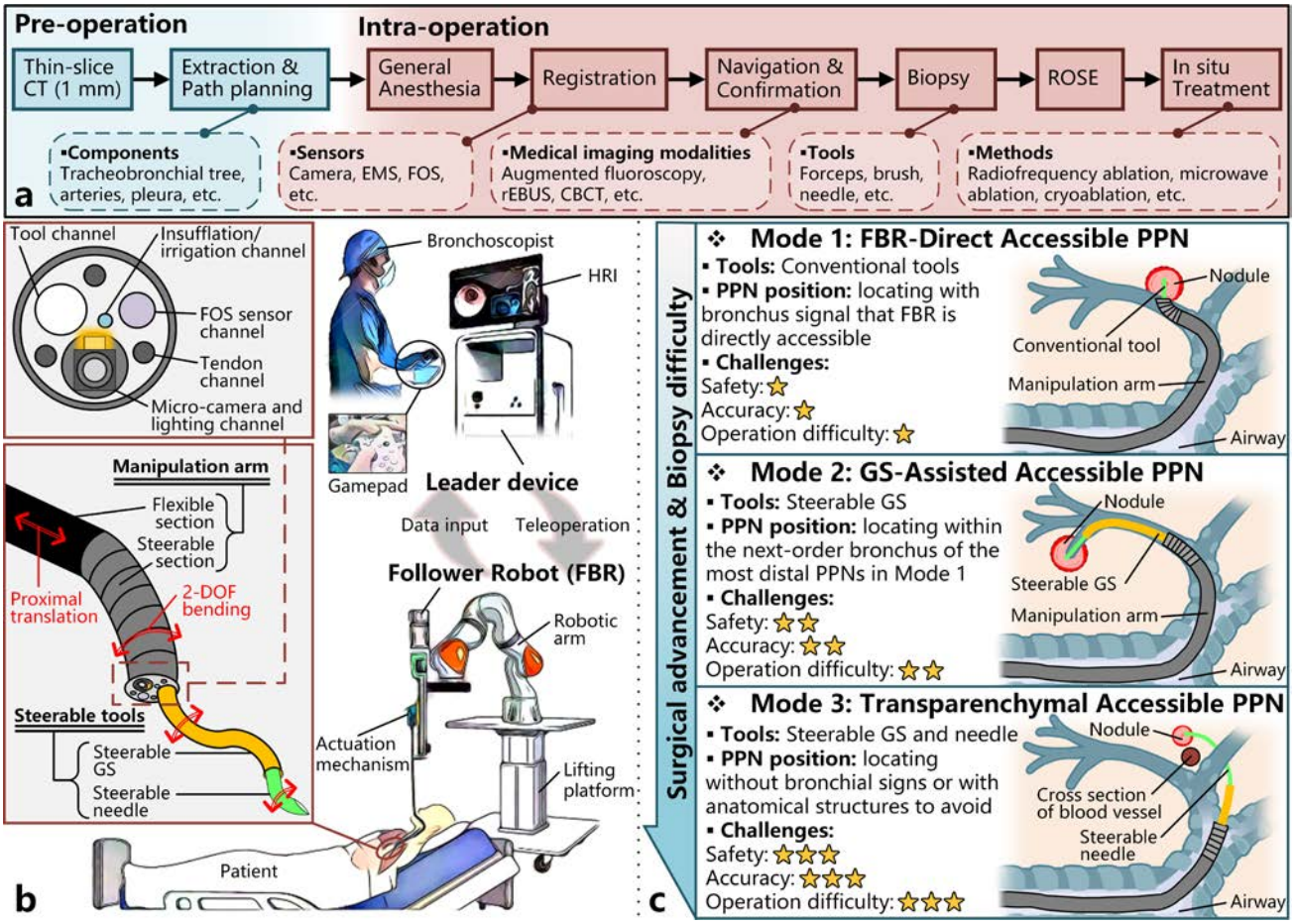

Fig. 3. Overview of the robotic-assisted bronchoscopy (RAB) system. (a) The flowchart illustrates the general procedure of the RAB. (b) The construction diagram shows the main components of a general RAB system and highlights a flexible bronchoscope robot (FBR) with exampled function and configuration. (c) FBR's deployment modes according to the locations of peripheral pulmonary nodules (PPNs). Abbreviations: CT, computed tomography; ROSE, rapid on-site cytological evaluation; rEBUS, radial-endobronchial ultrasound; CBCT, cone beam CT; EMS, electromagnetic sensor; FOS, fiber-optic sensor; GS, guide sheath; HRI, human-robot interface. Partly created with [44] and BioRender.com.

The robotic platform usually features a robotic arm with a lifting mechanism to adjust the FBR's posture. During the initial stage of the surgery, the platform is docked beside the patient, and the FBR is aligned with the introducer, which holds the endotracheal tube. The bronchoscopist then uses the controller to deploy the FBR into the bronchus.

B. Flexible Bronchoscope Robot and Inner Steerable Tools

FBR is the core of the RAB system. As presented in Fig. 3(b), it is typically a flexible-steerable continuum robot where the insertion part (manipulation arm) consists of a passive flexible body and an attached steerable section. This construction is necessary in distal airway navigation that requires high slenderness ratio [60]. The actuation system is located at the proximal end of the FBR, providing the translation and bending motion. Inner steerable tools are significant components to enhance FBR biopsy capabilities. They can be regarded as independent continuum robots for research purposes. For the sake of distinction and rigor in this review, the FBR and steerable tools (i.e., steerable GS and needles) are defined hereunder with both their medical and engineering characteristics:

1) Flexible Bronchoscope Robot: The FBR comprises an actuation mechanism and a manipulation arm. It is a flexible-steerable continuum robot with at least three inner channels: one for an embedded micro-camera and lighting system, another for insufflation/irrigation, and a third for assistive, biopsy, and therapeutic tools [61]. The detailed structure of a general FBR is shown in Fig. 3(b) with an enlarged view. Additional channels are often required for embedded EMS or FOS [62] and for tethered actuation mechanisms [63]. Due to the size constraints of the internal systems, the outer diameter of the FBR typically ranges from 2.4 to 4.4 mm [45], [64].

2) Steerable Guide Sheath: GS is a tube-like tool, which has been widely used in TBB, especially in EBUS with a GS (EBUS-GS) [65]. It serves as an extended tool channel beyond the bronchoscope's reach, allowing for repeated and accurate access to the nodule. Steerable GS achieves enhanced operability compared to GS by adding active bending degrees of freedom (DOFs). Additionally, it can serve as a guide tube to help the FBR traverse complex bronchi [66]. The outer diameter of the steerable GS is usually less than 2 mm for entering the tool channel.

3) Steerable Needle: Steerable needles were developed around two decades ago to enhance needle maneuverability

within tissue [67]. In TBB, the needle is commonly utilized for biopsy procedures such as fine needle biopsy and TBNA [68]. A steerable needle allows for precise steering through tissue, avoiding anatomical obstructions, and reaching PPNs without bronchial signs. The biopsy needle diameter is generally less than 1.1 mm (19G needle) for medical issues.

C. Deployment Modes of Flexible Bronchoscope Robot

As illustrated in Fig. 3(c), we outline three deployment modes for accessing PPNs featured with different anatomical locations. While each mode broadens the scope of biopsy, it also introduces challenges related to safety, accuracy, and operation. Below, we briefly describe the characteristics and challenges of each mode.

1) Deployment for FBR-Direct Accessible PPN: Several factors limit FBR's ability to reach the peripheral lung, including its diameter, steerability, operation skills, and availability of a safe path. These limitations restrict FBRs to reaching only some PPNs directly. Recent designs such as the mother-baby and ultra-thin configurations [69], [70] have expanded PPN accessibility, but deep advancement with FBRs worsens ergonomics.

2) Deployment for GS-Assisted Accessible PPN: Steerable GS enhances guidance, extending reach to the next generation of bronchi, but introduces operational and safety challenges due to the loss of built-in micro-camera vision. Due to the loss of visual feedback, the bronchoscopist is unable to deploy the GS using sensorimotor ability or estimate the contact force through tissue deformation, posing risks such as bronchus bleeding [71]. Additionally, in case of bleeding, detecting it promptly and safely positioning the tool for intervention may be challenging. The developments of supplementary intraoperative imaging and monitoring techniques may make this operation easier to perform [72], [73]

3) Deployment for Transparenchymal Accessible PPN: For nodules inaccessible via standard bronchoscopy—due to lack of bronchial signs or distance from bronchi—a transparenchymal approach with the steerable needle is required [74]. Although this method shows acceptable success rates in some studies [75], its accuracy is low for PPNs or nodules distance from the bronchi, due to the highly unpredictable needle-tissue interaction caused by tissue heterogeneity and lung dynamics. Moreover, safety concerns are significant for nodules near blood vessels. In recent years, advances in effective real-time needle tracking and precision steering have added value in further enabling this approach [76], [77].

III. Procedure-Specific Designs and Modeling

Advancements in continuum robotics have driven the development of FBRs and steerable GSs with structure and actuation designs suited to navigating the distal airways—characterized by narrow, fragile, highly branched, and sharply curved passages. The designs of FBRs and steerable GSs share core principles, which allow them to be discussed together in this section:

- Their structure and actuation are both integrated within a tube-like configuration for medical requirements;
- Their designs are constrained by the challenges of the peripheral airway environment mentioned above;
- They share common objectives, such as increasing stiffness, reducing diameter, and enhancing steerability.

Despite these shared principles, functional differences shape distinct design approaches. For example, while the concentric tube design suits steerable GS, it is less suitable for FBR, as the latter requires a passive flexible section at the proximal end [92].

In this section, we classify the state-of-the-art FBR and GS designs into tendon-driven notched, soft, and other designs, with recent advances summarized in Table I. Tendon-driven notched designs remain within the existing design paradigm, enhancing the performance of the FBR in distal airways through innovations in the structural design of the tube wall. Therefore, this design holds promise for rapid clinical translation. Soft designs, typically involving magnetic and fluid actuation, provide FBRs with inherent compliance and safety, while also enabling more advanced locomotion capabilities. Although clinical translation may not be feasible in the near term, FBRs with these designs hold considerable potential for future applications. Apart from the two mainstream designs, other designs, including concentric tube and multibackbone designs, have also been explored by some research groups with unique upsides. We also briefly review modeling methods for continuum robots and discuss their application in current FBR designs. Notably, although the steerable needle is also a critical component for design, it is deployed within the tissue, thus lacking FBR-related procedure-specific characteristics. Accordingly, it is rarely mentioned in this section.

A. Tendon-Driven Notched Designs

Tendon-driven continuum robots, the most prevalent type of continuum robots, operate by retracting tendons in the steerable section, causing the flexible backbone to bend due to the resulting bending moment. Due to the tube-like structure of the FBR and steerable tools, the advanced structural design involves carving hollow patterns into the tube-like surface, with precision laser cutting as the key fabrication method [66]. This is because laser cutting is mode-free and can directly cut millimeter-scale tubes into hollow patterns with micrometer precision. Notably, this method is vastly used in fabricating steerable needles due to their ultra-small diameters [93]. The cut tube is notched in the bending direction, which we refer to as the "tendon-driven notched design".

Initially, the tendon-driven notched design is hyper-redundant (i.e., non-continuum snake-like design), updating from manual version [94]. Its small-scale design is enabled by the assembly-free nature of the laser cutting method; the rotating pairs between joints self-assemble after laser cutting. Then, the compliant mechanism (CM) design is proposed that utilizes the laser to cut specially designed flexure hinges so that the tube acts as the central backbone of the continuum robot [81]. The hyper-redundant design achieves larger curvature than the CM design under the same steerable length, while this comes at the cost of potential danger in joint collision with the inner tube and outer environment.

TABLE I
SUMMARY OF RECENT ADVANCES IN FBR AND STEERABLE GS DESIGN

Reference	Features	Object	Fabrication[1]	Actuation	Diameter	Motion Pattern	Validation[2]
Tendon-Driven Notched Design							
[78] Gao 2020	Snake-like	Steerable GS	P; LC	FOS	2.2 mm	Bending	A
[79] Ai 2021	Multi-contact-aided CM	Steerable GS	P	Tendon	3.0 mm	Bending	P
[80] Bian 2023	Multi-section CM	FBR	LC	Tendon	3.5 mm	Bending	P
[81] Duan 2023	CM	FBR	—	Tendon	3.3 mm	Bending	P
[82] Ai 2024	paired cross-axis CM	Steerable GS	LC	Tendon	3.5 mm	Bending	P
Soft Design							
[83] Li 2022	Plastic balloon	FBR	L	Air	8.1 mm	Inchworm	PL
[64] McCandless 2022	Elastic cavity	FBR	C	Air	2.4 mm	Bending	PL
[70] Pittiglio 2023	Distributed magnets	Steerable GS	C	Magnetic field	2.0 mm	Follow-the-leader motion	CL
[84] Van Lewen 2023	Plastic membrane; balloon	FBR	C; L	Fluid	3.0 mm	Bending; inflation; origami	P
[85] Davy 2024	Soft growing design	FBR	Coating	Air	8.0 mm	Eversion	P
[69] Zhang 2024	Distributed magnets	baby FBR	Bonding	Magnetic field	2.0 mm	Bending	P
[86] Murasovs 2024	Magnetic tip	Steerable GS	LC; bonding	Magnetic field	2.0 mm	Bending	P
[87] Zhang 2024	Magnetic tip	mother-baby FBR	P; magnetic spray	Magnetic field	0.95 mm	Bending	PL
Other Design							
[88] Swaney 2017	Concentric tube	Steerable GS	—	Precurved tube	1.38 mm	Bending	PL
[89] Kato 2021	Multibackbone	FBR	—	Steel rod	3.0 mm	Bending; parallel motion	P
[90] Mitros 2021	Multibackbone	FBR	—	Ni-Ti rod	4.5 mm	Bending	P
[91] Wang 2024	Multibackbone	FBR	—	Ni-Ti rod	4.0 mm	Bending; elongation	P

Abbreviations: CM, compliant mechanism; FBR, flexible bronchoscope robot; FOS, fiber-optic sensor; GS, guide sheath.
[1]In this column: C, cast molding; L, lamination; LC, laser-cutting; P, 3-D printing.
[2]In this column: A, air; CL: cadaveric lung; P, phantom; PL, porcine lung.

Recent studies on CM design focus on developing and optimizing the tube patterns to fit the PPN biopsy environment. As shown in Fig. 4(a), Ai et al. developed a paired cross-axis design and increased the output stiffness of steerable GS by concentrically nesting two tubes [82]. Other related research includes multi-segment design to large steering angle [80] and multi-contact-aided design to anatomy-specific condition [95]. Despite the recent achievements, due to the effects of friction, material parameter uncertainty, and parasitic motion, elaborate statics and kinematics models for optimization and model-based control are still unsolved [60].

B. Soft Designs

1) Magnetically Actuated Soft Designs: Current studies related to magnetic actuation show increasing interest in magnetically tipped catheters and endoscopes [96]. The distal tip steers based on the magnetic torque or force generated by the embedded magnet under externally applied magnetic fields [97]. As the actuation is untethered, continuum robots can be designed to be very small (e.g., sub-millimeter scale) and free of transmission errors, which is unavoidable in tethered actuation. Therefore, in recent years, magnetic actuation has been widely adopted in intravascular applications [98] and endoscopic applications [99].

Thanks to the advances in soft magnetic material research [100], magnetically actuated soft design, i.e., bonding magnets into soft materials, has been developed in medical field to enhance the capability while maintaining safety, such as in arthroscopy [101]. In the context of FBR and steerable GS, Murasovs et al. parameterized the respiration cycle and presented a magnetically tipped steerable GS to compensate for the error by raising the navigation accuracy [86]. Compared to a single magnetic tip, a distributed magnet arrangement offers enhanced steerability and greater reliability. As shown in Fig. 4(b), Zhang et al. designed a mother-baby type FBR, and the baby FBR is soft and arranged with distributed magnets for actuation [69]. This aims to reduce the diameter and improve the flexibility. With a similar configuration, Pittiglio et al. focused on using multiple-point magnetic actuation to realize "follow-the-leader" deployment [70], [102] (the unchanged state of the curved shape of the body despite the advance of the tip [103]), and utilized dual-robot-arm approach to generate the required magnetic field [104]. Zhang et al. integrated advanced microscale 3-D printing and magnetic spray to fabricate an ultra-thin FBR. With an optical fiber array for imaging, the FBR achieves magnetic responsiveness with a 0.95 mm diameter [87].

While magnetic actuation enables ultra-miniaturized designs, the reduction in magnet size often compromises output stiffness. Consequently, this approach is more suitable

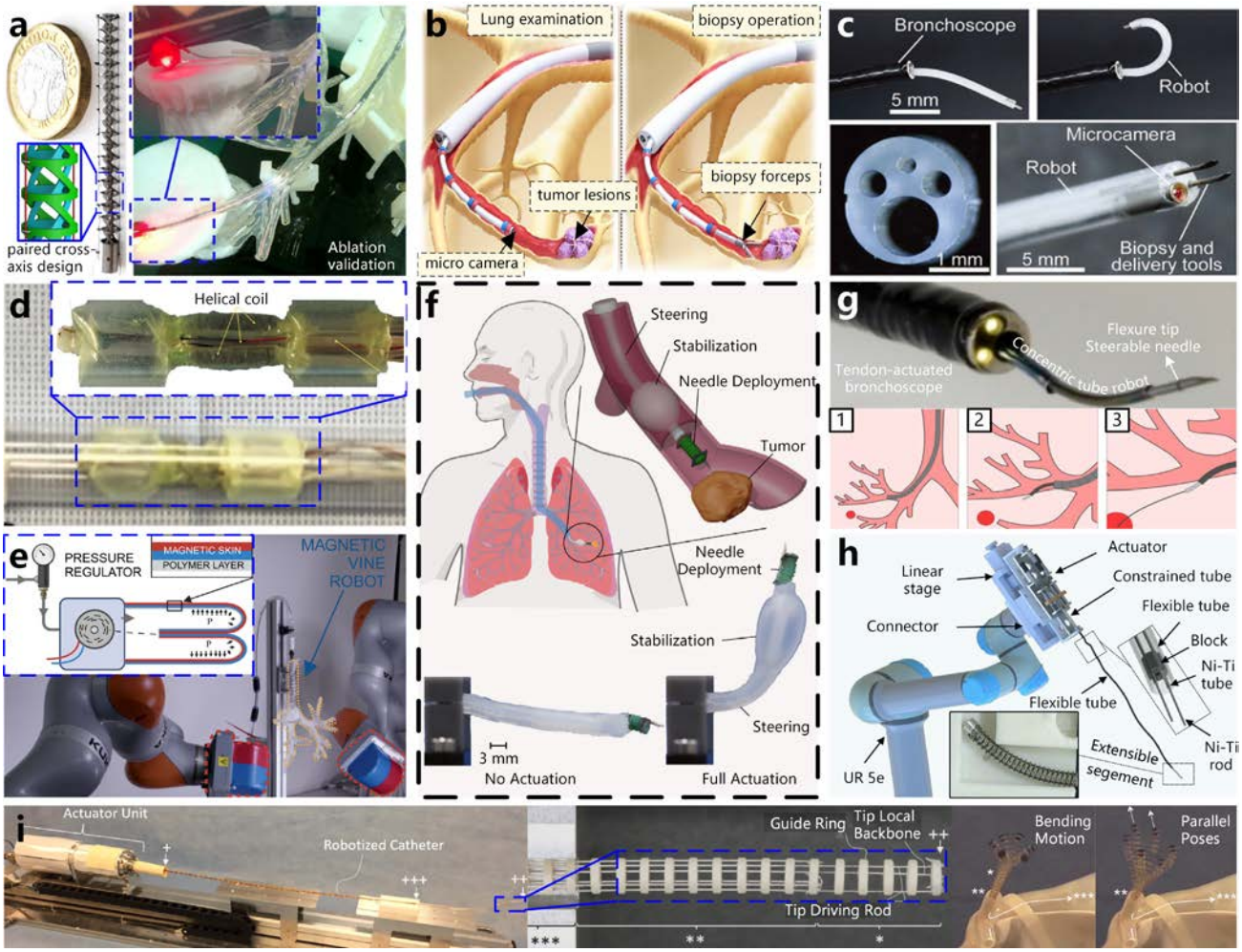

Fig. 4. State-of-the-art designs of flexible bronchoscope robot (FBR) and steerable guide sheath (GS). (a) Steerable GS with tendon-driven notched design by Ai et al. in [82]. The GS has a paired cross-axis structure for enhancing the output stiffness. (b) Magnetically actuated soft design of the baby FBR of a mother-baby type FBR by Zhang et al. in [69]. The magnets are distributed for diameter reduction and flexibility improvement. (c) FBR with fluid-driven soft design that integrates diagnosis and in situ treatment by McCandless et al. in [64]. (d) Self-propelled balloon FBR working in inchworm type by Li et al. in [83]. (e) Soft growing FBR with magnetic skin for enhanced steerability by Davy et al. in [85]. (f) Versatile FBR with fluid-driven soft design that integrates bending, stabilization, and needle deployment capabilities by Van Lewen et al. in [84]. (g) Steerable GS with concentric tube design for enhanced distal manipulation and deployment of an inner steerable needle for transparenchymal biopsy by Swaney et al. in [88]. (h) FBR with spring-like structure for direct tip extension by Wang et al. in [91]. (i) FBR with multi-segment multibackbone design for enhanced tip targeting (parallel pose) by Kato et al. in [89].

for developing steerable GSs or baby FBRs that demand enhanced flexibility; however, maintaining adequate output stiffness is critical to ensure the stability of internal tools during biopsy procedures. Furthermore, external manipulation systems, such as multi-axis electromagnets and robotic arms, remain a relatively large footprint, and their integration and spatial compatibility with existing bronchoscopy equipment warrant further investigation.

2) Fluid-Driven Soft Designs: Fluid-driven technology stands out as a leading and relatively mature technology in soft continuum robots, presenting a promising path toward earlier clinical translation compared to other soft actuation approaches [105]. Notably, fluid-driven soft designs enable advanced types of locomotion, offering significant advantages in enhancing the capability and safety of surgical tool deployment within confined spaces. For example, a soft continuum robot with extension-based actuation has been developed in transoral procedures [106]. In colonoscopy, eversion-based soft growing robot and robot with radial expansion ability have been explored [107], [108].

In the field of RAB, advanced locomotion strategies also facilitate access to PPNs, with some studies fundamentally redefining FBR's structural design. McCandless et al. introduced a pneumatic soft robot for combined biopsy and in situ treatment of PPNs (Fig. 4(c)), designed to function as either an ultra-small or a baby FBR with a diameter of 2.4 mm, though limited to a single actuation DOF [64]. To manage distal tip instability during proximal advancement of the FBR, Li et al. developed a self-propelled balloon FBR [83]. As depicted in Fig. 4(d), this design omits the passive flexible segment to transmit advance motion and employs an inchworm motion to directly advance the end, while the interaction safety between the FBR and distal airway requires further consideration.

Another approach to mitigate advance-induced uncertainty is through direct distal extension. In Fig. 4(e), Davy et al. proposed a soft growing robot (also known as vine robots)

for RAB, which incrementally added material at the tip by eversion [85]. They also embedded the magnetically active materials into the robotic surface so that the steerability could be improved without increasing the diameter. Additionally, Van Lewen et al. applied origami techniques to extend the distal tip directly, as shown in Fig. 4(f). They proposed a versatile soft robot with integrated bending, stabilization, and needle deployment capabilities [84]. Masking technique was used in combination with cast molding and lamination to fabricate the radially expansive soft actuator for stabilization and the bellows soft actuator (origami-inspired) for tip extension.

Beyond magnetic and fluidic actuation, recent work uses tendon-driven soft structures with low melting point alloys for temperature-controlled stiffness modulation [109]. Although FBRs with soft design have the potential to bring disruptive innovations to RAB procedures, soft robots are inherently challenging to model, which complicates navigation in complex environments. Moreover, miniaturization and surgical integration of endoscopic equipment remain pressing challenges that need to be addressed.

C. Other Designs

Robots featuring a concentric tube design consist of a series of pre-curved, thin, hollow telescoping tubes arranged concentrically, and actuated by translational and rotational motion at the proximal end [33]. Due to the actuation mechanism, this design is conducive to miniaturization but is only suitable for steerable GS [60]. For FBR, significant contributions to this field have been made by Kuntz, Webster III, and colleagues [88], [110]. As illustrated in Fig. 4(g), they proposed a steerable GS utilizing a concentric tube design integrated with a steerable needle as the end effector. Their contributions predominantly focus on advancing autonomous navigation and control, rather than the design. A detailed discussion of this will be provided in Section IV.

Multibackbone design has also been explored for FBR [89], [90], [91], [111]. Based on rod-based push-pull mechanisms, this configuration offers enhanced stiffness and fewer actuation DOFs compared to tendon-driven FBRs. As presented in Fig. 4(h), Kato et al. developed a FBR employing the multibackbone design. The robot has two bending sections that enable controlled dispersion for improving sampling opportunities [89]. As shown in Fig. 4(i), Wang et al. utilized the spring-like structure to design a multibackbone FBR with axial elongation ability [91], [111]. This enables the FBR to safely and easily access the peripheral lungs through a follow-the-leader motion strategy. However, the high stiffness of the passive flexure section, resulting from the multi-backbone design, must be considered in terms of its impact on the FBR's ability to conform to the airway. Additionally, limited mass-manufacturing processes must be considered for practical clinical applications.

D. Modeling Methods

In MIS, the modeling of continuum robots commonly relies on kinematic and static formulations due to the small size and safety-critical requirements. The modeling methods can be broadly classified into mechanics-based, geometric, discrete, and learning-based methods [30]. Among these, mechanics-based models are derived from continuum mechanics, typically under the slender-body assumption to enable reduced-order formulations. The Cosserat rod model, which represents the robot as a material line with continuously stacked rigid cross-sections, has served as a standard over the past decades. Geometric models, under the Cosserat assumptions, further simplify the robot's shape by constraining it to a predefined geometric curve. This eliminates the need to solve partial differential equations and allows static modeling using generalized coordinates derived from geometric assumptions. Although many candidate functions can describe the curves of continuum robots, the constant curvature (CC) assumption is most widely used due to its simplicity and compatibility with real-time control. Discrete models discretize the robot's configuration in the very beginning (e.g., lumped-mass or pseudo-rigid-body). They are easy to realize conceptually while requiring large efforts in parameter identification and model reduction for control purposes. Learning-based models are data-driven and independent of physical principles. While effective in simulation and control, they are limited for design purposes and often require large, task-specific datasets with limited generalizability across different robot types.

In the FBR domain, geometric models—particularly in CC assumptions—are most widely adopted [80], [81], [89], [94], [95], [111]. This is because most modeling efforts are intended to support closed-loop control, often accepting relaxed accuracy. For tendon-driven notched designs, simple design optimization based on the CC model is always performed. By applying static laws, mechanics-based CC models can also be derived for force estimation/control [112]. Mechanics-based models are generally necessary for soft designs. For magnetically actuated designs, mechanics-based models are used to map magnetic forces/torques to output motion [69], [85]. For fluid-driven designs, where fluid–structure interactions are strongly coupled, finite element methods are typically employed for design purposes [64], [84]. When addressing the more complex scenario of PPN biopsy, we believe that more realistic mechanics-based models, along with model reduction techniques, are needed. Notably, the Cosserat rod model has been rarely applied in current FBR studies; to the best of our knowledge, only [90] has adopted this approach. Recent developments in modeling fluid-driven soft robots, such as the "fluid Jacobian" [113], should be further translated into practical applications. Additionally, some studies have adopted discrete models for simplification [102], and learning-based methods for actuation error compensation [80].

IV. Autonomy-Enhanced Navigation and Control Strategies

Enhancing the autonomy of FBRs is an essential and inevitable progression, as it mitigates the impact of the robot's inherent ergonomic design limitations and, through the precision of robotic system perception and manipulation, bolsters the robot's capabilities in the peripheral lungs. While

TABLE II
DESCRIPTIVE CLASSIFICATION OF LOAS FOR FBR WITH EXAMPLES

Levels of Autonomy	Description	Examples
1: Robot guide	FBR acts as a guide for bronchoscopists by providing preoperative pathways and intraoperative guidance. The bronchoscopist requires continuous control of the FBR during the whole process (leader-follower operation).	1. Automatically generating preoperative pathway after manually choosing the PPN location. 2. Providing intraoperative navigation guidance by rendered virtual images or augmented reality.
2: Robot co-pilot	Based on LOA 1, FBR executes some assistive tasks during the continuous bronchoscopist's operation to improve operation accuracy and safety.	1. Continuous aligning scope location within the center of the lumen during navigation. 2. Assisting the bronchoscopist in steering toward the correct airway path during bifurcations.
3: Robot pilot	Based on LOA 2, FBR autonomously performs some subtasks under human decision-making to achieve hard tasks beyond human sensorimotor ability.	1. Safely navigating through distal airways with large curvature. 2. Locking the PPN site as a virtual remote center of motion and achieving precise advancement.
4: Supervisory autonomy	Based on the preoperative pathway and target location, the FBR can autonomously make decisions and execute subtasks.	1. Perceiving the navigation environment in real-time and making expert-level decisions. 2. Autonomously navigating along the global path and performing real-time path planning.
5: High & full autonomy	LOA 5 is a set that covers higher LOAs than LOA 4, which can not be achieved in the immediate future.	Advanced target recognition capabilities, such as detecting airway collapse, abnormal tissues, or airway bleeding, and autonomously managing these conditions.

increasing the autonomy of FBR offers clear benefits, it also significantly affects the risk management process, particularly as decision-making authority shifts from the bronchoscopist to the robot. Therefore, improving the research and development route to enhance the FBR's autonomy should be considered the first priority for the real implementation of high-autonomy systems. Building upon a high-performing FBR (as reviewed in Section III), the engineering challenges of enhancing autonomy primarily lie in improving the robot's navigation capabilities in the complex pulmonary environment and addressing human-robot shared control strategies under high-autonomy conditions.

In response to the aforementioned challenges, this section begins by defining the LOAs specifically for FBR with examples to refine the research roadmap. The definition is based on a balance of benefits and risks associated with each level, where increasing technical complexity corresponds to higher LOA. Next, we review recent advancements aimed at enhancing the navigation autonomy of FBRs, categorizing key stages into localization, motion planning, and execution. The discussion of execution primarily focuses on the human-robot shared control strategies.

A. Levels of Autonomy

Technical report IEC/TR 60601-4-1 [114] evaluates the LOAs in medical robots across four dimensions: monitoring, generating options, selecting options, and executing the option. It outlines several classification methods, such as descriptive techniques, binary classification, and weighting methods, to categorize LOAs. Then, Dupont et al. proposed an evolutionary framework for medical robot autonomy, describing six LOAs: no autonomy, robot assistance, task autonomy, conditional autonomy, high autonomy, and full autonomy [4]. In a related effort, Pore et al. applied a descriptive classification method typically to intraluminal and endovascular surgical robots, organizing them into five LOAs based on three navigation-related functions: target localization, motion planning, and execution/replanning [115]. They suggested that the next LOA for these robots would involve generating global paths and navigating autonomously to targets under supervision. However, these classifications are not directly transferable to FBRs. Unlike the scenarios described, FBRs already benefit from automated global preoperative motion planning. Yet, achieving supervised autonomy remains a multistage challenge requiring further development.

We adopt the descriptive method, enriched with specific examples, to define the LOAs tailored to FBRs. As outlined in Table II, we focus on defining and detailing the LOAs that FBRs can achieve in the near future, while offering only a limited description of FBRs with higher LOAs. LOA 1 represents current commercial FBRs in the form of leader-follower operations, which are undergoing clinical trials to evaluate their effectiveness. In LOA 2, navigation remains continuous operation of bronchoscopists. The robot functions as a co-pilot, assisting the bronchoscopist in tasks such as steering during airway bifurcations, thereby easing the operation difficulty and raising safety. In LOA 3, FBR can perform navigation sub-tasks step-by-step under the bronchoscopists' decision. Unlike LOA 2, FBR at this LOA operates independently of the bronchoscopist's sensorimotor skills during these sub-tasks. This LOA allows the robot to undertake more complex challenges, such as navigating sharp curvatures in distal airways. In LOA 4, decision-making authority shifts to the FBR, enabling it to complete navigation tasks under the supervision of bronchoscopists. This advancement requires precise dynamic perception of the surgical environment and the capability for intraoperative path replanning. LOA 5 represents the set of higher LOAs of FBRs. It surpasses LOA 4 by incorporating advanced target recognition capabilities, such as detecting airway collapse, abnormal tissues, or airway bleeding, and autonomously managing these conditions. Of note, although higher LOAs generally entail greater technical challenges, they may not fully align due to safety and ethical considerations. For instance, the LOA of FBR autonomously aligning the lumen should exceed that of autonomous entry

TABLE III
ADVANCES IN VISION-BASED LOCALIZATION, MOTION PLANNING, AND HUMAN-ROBOT CONTROL STRATEGIES FOR ENHANCING LOAS OF FBR

Vision-based localization strategies						
Reference	**Method**[1]	**Validation**	**Environment**[2]	**Bronchial generation**	**ATE**[3]	**Frequency**
[116] Sganga 2019	DL	ex-vivo (cadaver lung)	Partially dynamic	5th	≈8 mm	53.4 Hz
[117] Shen 2019	DL	in-vivo (patient data)	Dynamic	—	3.18±2.34 mm	0.35 Hz
[118] Zhao 2020	DL	in-silico (lung phantom)	Static	—	≈1.52 mm	11–13 Hz
[119] Banach 2021	DL	ex-vivo (porcine lung)	Partially dynamic	4th	6.2±2.9 mm	—
[120] Gu 2022	DRL	ex-vivo (porcine lung)	Dynamic	5th	8.62±1.19 mm	5 Hz
[121] Tian 2024	DL	in-vivo (porcine)	—	8th	N/A	51.8 Hz
Motion planning strategies						
Reference	**Category**[4]	**Object**	**Validation**	**Method**		**Real-time**
[122] Kuntz 2015	S	FBR & needle	—	Rapidly-exploring random tree (RRT)		N
[123] Fu 2018	S	Needle	in-vivo (human lung)	RRT & cost maps		N
[124] Hoelscher 2021	S	FBR & needle	ex-vivo (porcine lung)	RRT & backward planning		N
[125] Fu 2022	O	Needle	in-vivo (human lung)	Resolution optimality		N
[126] Bian 2024	L	FBR	—	Deep reinforcement learning		N
Human-robot shared control strategies						
Reference	**Method**		**Validation**	**Environment**[2]	**Goal**	**LOA**
[127] Sganga 2019	Preoperative trajectory tracking		in-silico (lung phantom)	Static	Global navigation	3
[128] Lin 2021	Augmented reality		in-silico (lung phantom)	Static	Enhanced information	1
[129] Zou 2022	Deep learning		in-silico (lung phantom)	Static	Steering & insertion	3
[70] Pittiglio 2023	Preoperative trajectory tracking		ex-vivo (cadaver lung)	Dynamic	Global navigation	3
[75] Kuntz 2023	Path replanning & sliding mode control		in-vivo (porcine)	Dynamic	Parenchymal steering	3
[130] Zhang 2024	Trained policy network		in-vivo (porcine)	Dynamic	Assisted insertion	2
[131] Van Lewen 2025	YOLO algorithm, sensor-based control		in-silico (lung phantom)	Static	Global navigation	3

Abbreviations: ATE, absolute trajectory errors; FBR, flexible bronchoscope robot; LOA, levels of autonomy; YOLO: you only look once.

[1]In this column: DL, deep learning; DRL, deep reinforcement learning.

[2]In this column: "dynamic" refers to under respiratory and airway deformation; "partially dynamic" refers to the absence of respiratory interference.

[3]ATE e_{ATE} is calculated by positional error e_p and angular error e_a by $e_{\text{ATE}} = \frac{e_p}{\cos(e_a)}$.

[4]In this column: S, sampling-based method; O, optimization-based method; L, learning-based method.

through the airway under human decision. The following subsections delve into current research aimed at advancing the LOAs of FBRs, including navigation and human-robot shared control strategies.

B. Autonomous Navigation

1) Localization: Bronchoscopic localization methods can be classified based on the type of sensors used: electromagnetic tracking with EMSs [132], shape sensing with FOSs [59], vision-based localization using micro-cameras, and hybrid approaches [133]. The EMS is integrated at the distal end of the FBR and generates voltage signals induced by the external magnetic field formed by the field generator. Current commercial systems achieve ideal orientation accuracy at sub-millimeter and sub-degree levels. However, the sensing accuracy is limited by the presence of metal or ferromagnetic sources within the operating workspace [134]. For FOS techniques, fiber Bragg grating (FBG) sensors are commonly used in FBRs to perform shape reconstruction, which relies on wavelength shifts caused by mechanical strain of sensor locations. However, large and complex deformations in FBR often require multiple fibers for adequate sensing accuracy, increasing both spatial footprint and system cost [62]. Vision-based localization offers significant advantages over EMS- and FOS-based methods. It requires no additional sensors and naturally filters respiratory interference caused by airway constraints [135], making it more cost-effective and less susceptible to CT-to-body divergence. In vision-based bronchoscopic localization, intraoperative video frames are typically registered with a preoperative airway model derived from CT scans. Various techniques, including intensity and gradient, have been developed to improve the accuracy of image registration [136], [137]. However, traditional computer vision techniques face challenges due to featureless and repetitive airway patterns, which limit localization accuracy and robustness. Furthermore, the registration speed of 1-2 Hz limits real-time control, impeding the progress of FBR towards achieving higher LOAs.

Recent advancements in learning-based approaches have enhanced visual-based bronchoscopic localization, offering the potential to meet higher precision. As shown in Table III, Sganga et al. introduced AirwayNet and BifurcationNet for real-time bronchoscope localization, improving the estimation of visible airways and their relative poses [116]. To improve robustness and mitigate artifacts, Shen et al. proposed a context-aware depth recovery method using a CycleGAN-like network, enabling direct depth estimation from bronchoscopic images [117]. Building upon this, Banach et al. developed 3cGAN, incorporated iterative closest point matching to register the estimated depth map and validated this approach systematically [119]. Instead of using deep learning solely

for depth estimation, Zhao et al. approached bronchoscopic localization as a learning-based global localization, replacing traditional CT-video registration [118]. Gu et al. considered robotic control signals as auxiliary inputs in their developed visual kinematic interaction framework, where the control signal is considered in the kinematic refinement networks to handle the kinematic imbalance [120]. Instead of coordinate-level localization, Tian et al. focused on branch-level estimation through lumen detection [121], offering increased real-time capabilities. Combining this with depth estimation methods may advance the current localization abilities.

2) Motion Planning: Motion planning methods for FBRs are largely preoperative and rely on segmented bronchial trees. These methods fall into four categories: node-based, sampling-based, optimization-based, and learning-based techniques [115], [138]. Early approaches, such as node-based planning, assisted bronchoscopists in navigating complex airway structures [139]. However, these methods treated airways as rigid, limiting their application in the dynamic environment of distal airways. Sampling- and optimization-based methods, designed to account for FBR-specific characteristics, have made significant strides in ensuring safe and accurate motion planning in distal airways. Alterovitz's team has made notable contributions in this area based on a developed concentric tube-type FBR (Fig. 4(g)) with three-stage deployment strategies [122], [123], [124], [125]. As presented in Table III, Kuntz et al. developed a sampling-based motion planner that integrates three deployment stages in a unified algorithm, explicitly considering the coupling across different stages [122]. To enhance computational speed, Hoelscher et al. proposed a backward planning strategy, reversing the problem by constructing a needle search tree from the target location [124]. For steerable needle deployments, Fu et al. developed a method for automatically extracting cost maps from CT images to efficiently plan safe motions [123]. They also proposed an optimization-based approach that generates higher-quality plans through defined "resolution optimality" [125]. Despite these advances, sampling- and optimization-based methods continue to face challenges in the compromise between the computation time and the optimal path. Learning-based methods have shown their advantages in other robotic-assisted MIS procedures with higher LOAs, including liver, vessel, and colon environments [140], [141], [142]. In the RAB scenario, to the best of the authors' knowledge, only Bian et al. proposed a learning-based motion planning algorithm that aims to enable autonomous intervention for deep and tortuous bronchial pathways based on the developed few-human-interaction twin-delayed deep deterministic policy gradient [126]. Most current motion planning methods are preoperative. However, to enhance the autonomy of FBR, intraoperative real-time motion planning is essential to provide accurate paths for high-level controllers. Learning-based approaches present a promising solution, though challenges such as safety concerns and the need for vast amounts of training data must be addressed.

3) Simulation Environment: The simulation environment plays a crucial role in advancing autonomous navigation, especially when learning-based methods are involved. The virtual airway is typically generated by segmenting CT images using software such as 3D Slicer. Other components of the simulation environment depend on the task, for example, vision-based localization usually requires only a virtual camera and motion paths, while simulating full navigation necessitates a virtual FBR integrated with kinematics. Notably, virtual airways have long been employed in virtual bronchoscopic navigation [50], and virtual FBR has also been used in computational path planning [122]. In learning-based approaches, simulation environments are often utilized to generate datasets due to the difficulty of collecting real-world data. However, transferring knowledge from simulation to real-world scenarios remains a major challenge, i.e., the "sim-to-real" gap.

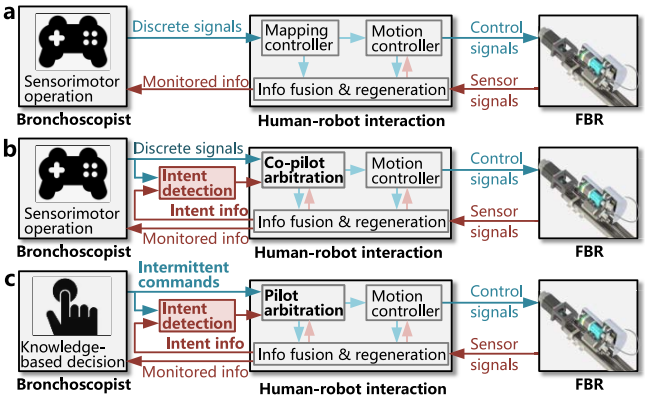

Fig. 5. Human-robot shared control evolution in flexible bronchoscope robots (FBRs). (a) Conventional control framework for leader-follower mode. (b) FBR co-pilot mode, where intent detection and arbitration are introduced. (c) FBR pilot mode, where bronchoscopists' sensorimotor operation is transferred to the knowledge-based decision.

Recent studies have explored techniques to reduce this gap. Methods including domain randomization [126], [143], domain adaptation [120], [130], fine-tuning [144], and data augmentation [118], [130] are developed to enhance the generalization capability. However, these methods still offer limited robustness against real-world variability and introduce additional computational cost. Real-time capability is also critical to reduce the sim-to-real gap. It ensures time-consistent feedback during the training and testing of autonomous policies, particularly in closed-loop interactions. Some advanced registration techniques, such as the gradient-based method [137] and depth-based method [145], have been proposed to improve real-time performance in localization. Some developed real-time physical simulation frameworks (e.g., SOFA [144]), also contribute significantly to establishing a real-time simulation environment for FBR navigation.

C. Human-Robot Shared Control

The human-robot shared control strategies are intrinsically linked to the LOAs proposed in Section IV-A. This subsection outlines the general evolution of human-robot shared control frameworks designed for FBRs operating at LOAs 1–3, as depicted in Fig. 5. The state-of-the-art works are summarized in Table III and discussed hereafter. A comprehensive summary of state-of-the-art studies is presented in Table III

and further elaborated upon hereinafter. Notably, an increase in LOA does not inherently imply greater complexity in control technologies but rather reflects a paradigm shift in human-robot collaboration.

Figure 5(a) illustrates the prevailing collaboration paradigm at LOA 1, wherein bronchoscopists teleoperate FBRs via a joystick without assistance (leader-follower model). This paradigm relies heavily on the operator's sensorimotor skills, particularly hand-eye coordination, due to the absence of tactile feedback in current systems. The human-robot interaction at this level involves mapping the bronchoscopist's discrete inputs to corresponding shape configurations, which are processed by a motion controller. Typically, the motion controller operates on two levels: a high-level controller for shape tracking and a low-level controller for joint-level control. Alternatives like hybrid motion/force controllers are conceivable; however, the details of specific control algorithms of these controllers are beyond the scope of this subsection. For instance, human-robot interaction integrates and regenerates various sensory signals, operational inputs, and control variables to provide real-time control feedback (e.g., shape reconstruction via FOS) and monitored information (e.g., rendered virtual imagery). For instance, Lin et al. introduced an augmented reality-assisted system that integrates an EMS, FOSs, and a head-mounted display to create an immersive experience for bronchoscopists [128], [146]. Gesture recognition technology has also been explored as a joystick replacement to enhance operational convenience.

At LOA 2, the introduction of intent detection and co-pilot arbitration marks a significant evolution toward a collaborative framework, wherein the FBR assumes a co-pilot role [147]. Intent detection identifies the procedural step, although most current methods rely on explicit operator input. Co-pilot arbitration synthesizes control signals from both the human operator and the robot. Crucially, the FBR must accurately define the current task based on the environment and the operational inputs. Simultaneously, the robot should enhance the safety and efficiency of peripheral lung navigation by addressing environmental challenges, such as dynamic disturbances and airway constraints, which contribute to instability during operations. Zhang et al. proposed an artificial intelligence (AI)-human shared control algorithm to minimize tissue damage while maintaining efficiency [130]. The core of the algorithm is a policy network that uses a bronchoscopic image and a discrete human command to predict the robot's steering action. They also developed a shared control strategy using the Unet model for cavity segmentation, enabling co-control of the robot to navigate into the correct cavity [148].

At LOA 3, the FBR assumes pilot control, performing challenging sub-tasks under the bronchoscopist's determination. The FBR receives intermittent commands from the bronchoscopist to execute appointed sub-tasks. The greatest merit of LOA 3 is that the FBR can perform sub-tasks without relying on the bronchoscopist's sensorimotor ability. Unlike LOA 2, the FBR and the bronchoscopist in this framework operate independently, with task decisions guided by the bronchoscopist's medical expertise. Therefore, the intent detection and arbitration of LOA 3 are simpler than those in LOA 2. The key matters in LOA 3, in addition to establishing a tailored control framework, are to develop control strategies that enable the FBRs to exceed human capabilities in executing specific sub-tasks. For instance, McCandless et al. mentioned in their research that they developed an image-based mechanism to align the lumen center [64], which is one of the simplest sub-tasks. Zou et al. combined histogram back-projection and deep learning-based methods to detect the lumen center with high robustness and accuracy for automatic steering and insertion [129]. Some studies use a preoperatively generated path trajectory as the reference for path tracking controllers, enabling global autonomous navigation without the need for decision-making during the procedure. Sganga tested a proportional controller for global navigation in phantom lungs, but the error exceeded 10 mm [127]. Pittiglio et al. evaluated a magnetic soft FBR in cadaver lungs with disturbances, using a preoperative-derived pathway to generate predetermined optimal actuation fields for autonomous navigation [70]. Van Lewen et al. developed a semi-autonomous soft FBR platform that employs a YOLO-based algorithm for branch detection, with closed-loop control enabled by onboard vision and EMS feedback [131]. Webster III's team focused on autonomous needle steering to reach PPNs. Kuntz et al. replanned the trajectory before initiating the steering process and used intermittent operation to mitigate respiratory effects [75]. In addition, Hoelscher et al. introduced a start pose robustness metric to assess the impact of small human–robot handoff deviations, enabling the selection of navigation plans with larger safe start regions [149]. Despite the efforts made in the aforementioned studies, real-time path planning and intraoperative perception are essential for achieving precise and safe global autonomous navigation.

Current research has not yet explored the LOA 4. At this level, the FBR functions similarly to a "bronchoscopist", capable of independently making decisions and completing navigation under supervision. The real bronchoscopist monitors the robot's actions and can take over at any time. Therefore, shared control at this level should transition to "shared autonomy" [150], enabling dynamic adjustment of human-robot autonomy through the development of adaptive autonomy methods. Control strategies at higher LOAs may fall outside the realm of human-robot collaboration and are therefore not discussed in this review.

V. Future Directions

We have witnessed the momentum of FBR during its first decade, characterized by promising initial clinical outcomes of commercial products and the mixed sentiments of bronchoscopists, including both encouragement and concerns. Additionally, we have observed that advancements in soft and continuum robotics, AI-enhanced navigation and control methods, etc., have subtly influenced the emergence of next-generation FBRs in the academic arena, aimed at fulfilling the aspirations of bronchoscopists for a significant role in the early diagnosis and possible treatment of lung cancer. In the following discussion, we explore the clinical objectives that next-generation FBR is expected to achieve from the

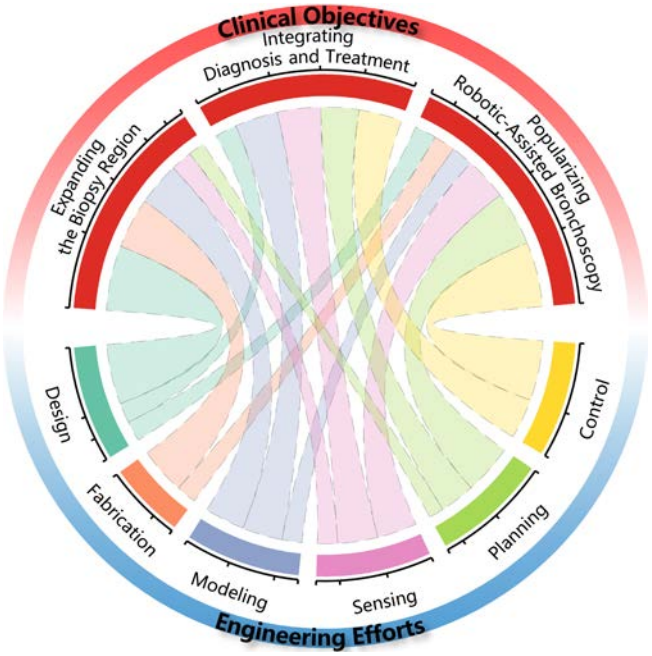

Fig. 6. Chord diagram qualitatively illustrating the engineering efforts required in flexible bronchoscope robots to achieve advanced clinical objectives.

practitioner's perspective, using these objectives as subheadings. For each clinical objective, we discuss the engineering efforts required by researchers to support their realization. The qualitative relationships are depicted in Fig. 6.

A. Expanding the Biopsy Region

The limited biopsy range of RAB constrains its application and is a key factor preventing it from fully replacing TBB. Existing research has made certain efforts to expand the range of RAB; however, further advancements are still required to reduce the diameter to access higher-generation airways and improve steerability to pass tortuous airways. We suggest using "outer diameter" and "steerability" (typically represented by curvature and steering angle) rather than airway generation as metrics to evaluate the performance of FBR in engineering or biomedical engineering research. This is because airway generation is a patient-specific parameter unless it holds statistical significance in the context of the study.

The miniaturization of FBRs is currently limited by clinical requirements for inner tool channels (1.2–2.8 mm) and the dimensions of integrated sensors, such as micro-cameras with diameters ranging from 0.8 to 1.6 mm, resulting in an outer diameter of approximately 3 mm. Consequently, further miniaturization necessitates advancements in reducing the size of both the required tools and embedded sensors. Magnetic actuation is capable of small size, while the size and compatibility of the peripherals need to be considered, as well as providing sufficient intervention force. For fluid-driven soft robots, miniaturization remains challenging, particularly in the context of multifunctionality, due to limitations in design and fabrication techniques. Based on the given structural configuration, model- and computational path planning-based optimization may enhance the FBR's performance, while the latter must solve the problem of generalization.

Enhancing steerability is also crucial for expanding the biopsy range. While currently developed FBRs are reported with large steering angles (140°-210°), the axial length of steerable sections is not significantly restricted. This means the maximum curvature, an important measure of steerability, is seldom addressed in current research [64], [80], [85], [102], and its consideration is recommended in future studies. Further progress in steerability involves replacing traditional proximal advancement and distal bending with advanced locomotion patterns such as inchworm motion [83], distal anchoring [84], and follow-the-leader deployment [91]. These innovative locomotion patterns can mitigate the impact of unknown airway constraints during insertion or steering, facilitating easier access to the peripheral lung regions.

Additionally, some PPNs may lack bronchial and vascular signs, complicating navigation and biopsy. This challenge may be addressed by developing steerable needle-based transparenchymal biopsies [67], [75] or combining advanced navigation techniques (e.g., AI-enhanced SLAM) to reach PPNs in unknown environments. The former's key challenge lies in needle steering within tissues, which falls outside the scope of FBR research.

B. Integrating Diagnosis and Treatment

The benefits of using bronchoscopy technology to integrate the diagnosis and treatment of PPNs are evident. In contrast to traditional methods such as surgical resection or stereotactic body radiotherapy, the direct use of bronchoscope for both diagnosis and treatment within a single procedure presents a safer, more efficient, and cost-effective solution [57]. In addition, recent studies have demonstrated that RAB can biopsy lymph nodes in traditionally inaccessible regions such as the aortopulmonary window (stations 5 and 6) [151], [152], enhancing its utility for staging. Moreover, advanced bronchoscopy-based in situ ablation techniques, including microwave and radiofrequency ablation, have shown promising results [153], [154]. Consequently, the development of integrated diagnostic, staging, and therapeutic technologies based on RAB is not only technically feasible but also of considerable clinical importance [6].

The integration of diagnosis and treatment in FBRs depends on three critical factors: achieving reliable diagnosis, developing safe surgical procedures, and demonstrating therapeutic effectiveness. From an engineering standpoint, FBR research must overcome challenges in achieving precise targeting of pulmonary nodules and lymph node stations and facilitating multi-site navigation within a single procedure.

Current RAB procedures reveal a mismatch between navigation success and diagnostic accuracy [46]. This is mainly due to CT-to-body divergence—FBRs are unable to accurately obtain intraoperative positions of the robot and nodules from preoperative CT due to factors such as respiration, atelectasis, and tissue deformation. Although recent advances based on machine learning methods have integrated preoperative image data and developed real-time localization algorithms to track the FBR tip and biopsy tools, the information about the bronchial tree map and nodules predominantly resides in prior or posterior knowledge. Therefore, to ensure biopsy accuracy,

new algorithms based on visual or other intraoperative sensory information need to be developed to perceive the dynamic changes in the bronchial tree and PPNs, enabling local map updates and path replanning. For example, a feasible approach may involve acquiring real-time 2-D ultrasound images of the bronchial wall and surrounding tissues through rEBUS, followed by reconstructing these 2-D images into localized 3-D structures using learning-based algorithms to assist in identifying the location of target nodules. To achieve this, it is first necessary to develop a simplified FBR-specific airway tree model based on airway morphological features, obtained through secondary processing of bronchial tree image segmentation. In advanced studies, Kuntz et al. considered respiratory factors and achieved better results than manual bronchoscopy through intermittent tool advancement and path replanning [75]. Although some targeting errors in in-vivo porcine tests are unacceptable (e.g., 10.2 mm), their studies prove the correctness of this development path.

Precise targeting of dynamic targets is essential while challenging in the procedure of integrating diagnosis and treatment. Respiratory-induced target position shifts in the lungs can reach up to 20 mm (e.g., in the right lower lung), which is unacceptable for small pulmonary nodules and lymph nodes requiring biopsy, typically ranging from 5 to 20 mm in size. In situ treatment procedures require higher positional precision than biopsy, particularly for larger lesions. The limited scope of local treatment necessitates accurate needle placement at the nodule's center to achieve complete ablation and reduce the risk of recurrence. In such scenarios, advanced model-based or data-driven closed-loop control strategies must be developed to enhance the autonomy of FBRs, providing effective assistance to bronchoscopists. For instance, when targeting a nodule, the target can be treated as a moving remote center of motion point, introducing control constraints to reduce the operational complexity for the bronchoscopist. Alternatively, advanced path-tracking algorithms can be designed to directly reach the target. A significant challenge in these studies lies in the dynamic constraints imposed by the airway walls on the FBR, which are often unperceived and hard to model, severely impacting control stability and precision. In addition, advanced structural designs enabling leader-follower motion and distal biopsy enhancement can reduce control complexity while improving targeting accuracy [89].

Furthermore, as the integration of diagnosis and treatment involves multi-site navigation within a single procedure, the occurrence of complications increases proportionally with the number of navigation attempts, necessitating a reassessment of safety concerns. One key issue is whether the FBR can perform measures in regions where manual operation is challenging, either autonomously or with human assistance, such as compression hemostasis for common complications like bleeding. This introduces higher demands for real-time path planning in FBR.

C. Popularizing Robotic-Assisted Bronchoscopy

With the widespread adoption of lung cancer screening programs, the detection of pulmonary nodules has increased significantly. While established evaluation systems for malignant pulmonary nodules are in place, conducting a reliable biopsy without the risks associated with surgery is crucial to not only meeting patients' psychological needs but also enabling earlier identification of cancerous nodules. RAB has demonstrated its considerable promise in facilitating precise and safe biopsy procedures, even in the peripheral regions. However, the widespread adoption of RAB procedures faces significant challenges: the shortage of experienced bronchoscopists and the unequal distribution of medical resources.

One solution to address the shortage of experienced bronchoscopists in current research is to integrate 5G technology for remote robotic surgeries [155]. However, while this approach can help balance medical resources across regions, it does not increase the overall number of bronchoscopists capable of performing RAB procedures. A promising avenue lies in enhancing the LOAs of the FBRs, which would help mitigate the learning curve for operators. With the assistance of a robotic co-pilot or pilot, bronchoscopists of varying experience levels can operate the system with comparable proficiency, even surpassing their original capabilities.

Second, cost reduction is essential to promote the RAB procedure. Engineering solutions to address this primarily focus on the following aspects. For the actuation system, given the current high cost of magnetic actuation systems, their manufacturing expense remains a barrier to widespread adoption. Sensor systems represent a significant cost burden for FBR, especially the accurate FOS, necessitating the development of navigation and control technologies based solely on built-in cameras. The fabrication and maintenance of FBRs should also be considered. The Galaxy platform employs a single-use bronchoscope, with only the camera being reusable, thereby reducing the fabrication and maintenance expenses. For tendon-driven notched design, precision injection molding technology holds promise as a replacement for laser cutting in manufacturing. The relatively low manufacturing cost of soft robots, coupled with advancements in manufacturing technologies, offers the potential to achieve complex design types at a lower cost.

VI. Conclusion

Over the past decade, RAB has emerged and rapidly evolved in response to the growing need for PPN management and the continuous advancement of continuum robotics. This review presents an engineering-focused overview of recent advancements in FBRs. To clarify the associated engineering challenges, we first introduced the clinical background and provided a simplified overview of RAB systems. Key developments in FBRs were then summarized from two perspectives: patient-specific design and modeling, and autonomy-enhanced navigation and control. Technical solutions were comparatively analyzed with a focus on their relevance to PPN intervention. We also provided a description of the LOAs for FBRs to help refine the roadmap toward higher LOAs.

Our review indicates that some engineering efforts may overlook practical surgical considerations, which could hinder clinical translation. To address this gap, we distilled key clinical concerns and expectations from recent studies and

used these insights to inform future directions for FBR development. Emphasis was placed on evaluating engineering efforts that support the future directions. We hope this review serves as a valuable reference for researchers aiming to advance clinically meaningful FBRs in the evolving landscape of continuum robotics.

REFERENCES

[1] V. Vitiello, S. L. Lee, T. P. Cundy, and G. Z. Yang, "Emerging robotic platforms for minimally invasive surgery," *IEEE Rev. Biomed. Eng.*, vol. 6, pp. 111–126, 2013.

[2] Y. Wang et al., "Bioinspired handheld time-share driven robot with expandable DoFs," *Nat. Commun.*, vol. 15, no. 1, p. 768, 2024.

[3] J. Rogatinsky et al., "A multifunctional soft robot for cardiac interventions," *Sci. Adv.*, vol. 9, no. 43, 2023, Art. no. eadi5559.

[4] P. E. Dupont et al., "A decade retrospective of medical robotics research from 2010 to 2020," *Sci. Robot.*, vol. 6, no. 60, 2021, Art. no. eabi8017.

[5] N. Kurimoto, "Robotic-assisted bronchoscopy approaches for peripheral pulmonary lesions," *Respirology*, vol. 28, no. 1, pp. 15–16, 2023.

[6] E. H. F. M. van der Heijden and R. L. J. Verhoeven, "Robotic assisted bronchoscopy: The ultimate solution for peripheral pulmonary nodules?" *Respiration*, vol. 101, no. 5, pp. 437–440, 2022.

[7] J. D. D. Duke and J. Reisenauer, "Robotic bronchoscopy: Potential in diagnosing and treating lung cancer," *Exp. Rev. Resp. Med.*, vol. 17, no. 3, pp. 213–221, 2023.

[8] A. A. Thai, B. J. Solomon, L. V. Sequist, J. F. Gainor, and R. S. Heist, "Lung cancer," *Lancet*, vol. 398, no. 10299, pp. 535–554, 2021.

[9] R. L. Siegel, A. N. Giaquinto, and A. Jemal, "Cancer statistics," *Cancer J. Clinicians*, vol. 74, no. 1, pp. 12–49, 2024.

[10] S. J. Adams, E. Stone, D. R. Baldwin, R. Vliegenthart, P. Lee, and F. J. Fintelmann, "Lung cancer screening," *Lancet*, vol. 401, no. 10374, pp. 390–408, 2023.

[11] J. Burgei, K. Alsheimer, and B. Hehn, *Carcinoid and Adenocarcinoma Diagnosed With Robotic-Assisted Bronchoscopy*, Amer. Thoracic Soc., New York, NY, USA, 2023, pp. A4141–A4141.

[12] G. A. Silvestri et al., "An evaluation of diagnostic yield from bronchoscopy," *Chest*, vol. 157, no. 6, pp. 1656–1664, 2020.

[13] N. Navani et al., "Lung cancer diagnosis and staging with endobronchial ultrasound-guided transbronchial needle aspiration compared with conventional approaches: An open-label, pragmatic, randomised controlled trial," *Lancet Resp. Med.*, vol. 3, no. 4, pp. 282–289, 2015.

[14] G. J. Criner et al., "Interventional bronchoscopy," *Amer. J. Resp. Crit. Care Med.*, vol. 202, no. 1, pp. 29–50, 2020.

[15] J. Kim, C. G. Chee, J. Cho, Y. Kim, and M. A. Yoon, "Diagnostic accuracy and complication rate of image-guided percutaneous transthoracic needle lung biopsy for subsolid pulmonary nodules: A systematic review and meta-analysis," *Brit. J. Radiol.*, vol. 94, no. 1127, 2021, Art. no. 20210065.

[16] D. M. DiBardino, L. B. Yarmus, and R. W. Semaan, "Transthoracic needle biopsy of the lung," *J. Thoracic Disease*, vol. 7, no. S4, p. S304, 2015.

[17] K. Walter, "Pulmonary nodules," *J. Amer. Med. Assoc.*, vol. 326, no. 15, pp. 1544–1544, 2021.

[18] M. Chafkin. "Robots could replace surgeons in the battle against cancer." 2018. [Online]. Available: https://www.bloomberg.com/news/features/2018-03-23/robots-could-replace-surgeons-in-the-battle-against-cancer.

[19] Intuitive Surgical. "How ion works." 2024. [Online]. Available: https://www.intuitive.com/en-us/products-and-services/ion/how-ion-works.

[20] "Noah Medical." 2025. [Online]. Available: https://www.noahmed.com/galaxy-system-walkthrough

[21] V. Anderson and R. Horn, "Tensor arm manipulator design," *Trans. ASME*, vol. 67, pp. 1–12, Nov. 1967.

[22] T. Miyazawa, "History of the flexible bronchoscope," in *Interventional Bronchoscopy*. Basel, Switzerland: Karger, 2000, pp. 16–21.

[23] P. J. Swaney et al., "Tendons, concentric tubes, and a bevel tip: Three steerable robots in one transoral lung access system," in *Proc. IEEE Int. Conf. Robot. Autom. (ICRA)*, 2015, pp. 5378–5383.

[24] C. Wright et al., "Design of a modular snake robot," in *Proc. IEEE/RSJ Int. Conf. Intell. Robots Syst.*, 2007, pp. 2609–2614.

[25] C. Wright et al., "Design and architecture of the unified modular snake robot," in *Proc. IEEE Int. Conf. Robot. Autom.*, 2012, pp. 4347–4354.

[26] I. Webster, J. Robert, and B. A. Jones, "Design and kinematic modeling of constant curvature continuum robots: A review," *Int. J. Robot. Res.*, vol. 29, no. 13, pp. 1661–1683, 2010.

[27] D. C. Rucker and R. J. Webster, "Statics and dynamics of continuum robots with general tendon routing and external loading," *IEEE Trans. Robot.*, vol. 27, no. 6, pp. 1033–1044, Dec. 2011.

[28] R. J. Webster, J. M. Romano, and N. J. Cowan, "Mechanics of precurved-tube continuum robots," *IEEE Trans. Robot.*, vol. 25, no. 1, pp. 67–78, Feb. 2009.

[29] M. Russo et al., "Continuum robots: An overview," *Adv. Intell. Syst.*, vol. 5, no. 5, 2023, Art. no. 2200367.

[30] C. Armanini, F. Boyer, A. T. Mathew, C. Duriez, and F. Renda, "Soft robots modeling: A structured overview," *IEEE Trans. Robot.*, vol. 39, no. 3, pp. 1728–1748, Jun. 2023.

[31] M. Tummers, V. Lebastard, F. Boyer, J. Troccaz, B. Rosa, and M. T. Chikhaoui, "Cosserat rod modeling of continuum robots from Newtonian and Lagrangian perspectives," *IEEE Trans. Robot.*, vol. 39, no. 3, pp. 2360–2378, Jun. 2023.

[32] S. Lilge, K. Nuelle, J. A. Childs, K. Wen, D. C. Rucker, and J. Burgner-Kahrs, "Parallel-continuum robots: A survey," *IEEE Trans. Robot.*, vol. 40, pp. 3252–3270, 2024.

[33] C. J. Nwafor, C. Girerd, G. J. Laurent, T. K. Morimoto, and K. Rabenorosoa, "Design and fabrication of concentric tube robots: A survey," *IEEE Trans. Robot.*, vol. 39, no. 4, pp. 2510–2528, Aug. 2023.

[34] C. Zhang, F. Xie, R. Li, N. Cui, F. J. F. Herth, and J. Sun, "Robotic-assisted bronchoscopy for the diagnosis of peripheral pulmonary lesions: A systematic review and meta-analysis," *Thoracic Cancer*, vol. 15, no. 7, pp. 505–512, 2024.

[35] F. Pyarali, N. Hakami, and G. E. Chaux, "Meta analysis of diagnostic yield and complications with robotic-assisted navigation bronchoscopy," *Chest*, vol. 162, no. 4, 2022, Art. no. 2115A.

[36] M. S. Ali, U. K. Ghori, M. T. Wayne, E. Shostak, and J. De Cardenas, "Diagnostic performance and safety profile of robotic-assisted bronchoscopy a systematic review and meta-analysis," *Ann. Amer. Thoracic Soc.*, vol. 20, no. 12, pp. 1801–1812, 2023.

[37] D. Abia-Trujillo et al., "Mobile cone-beam computed tomography complementing shape-sensing robotic-assisted bronchoscopy in the small pulmonary nodule sampling: A multicentre experience," *Respirology*, vol. 29, no. 4, pp. 324–332, 2024.

[38] A. C. Chen and C. T. Gillespie, "Robotic endoscopic airway challenge: Reach assessment," *Ann. Thoracic Surg.*, vol. 106, no. 1, pp. 293–297, 2018.

[39] U. Chaddha et al., "Robot-assisted bronchoscopy for pulmonary lesion diagnosis: Results from the initial multicenter experience," *BMC Pulmonary Med.*, vol. 19, no. 1, p. 243, 2019.

[40] A. H. Alraiyes, A. R. Cedeno-Rodriguez, G. W. Chmielewski, and A. W. Joob, "The outcome of the same anesthesia event for robotic bronchoscopy marking and robotic sub-lobar resection of lung nodules," *Chest*, vol. 164, no. 4, 2023, Art. no. 4238A.

[41] M. Schneider, N. G. Wysham, and S. Kotova, "Shape-sensing robotic-assisted bronchoscopy and robotic segmentectomy," *Chest*, vol. 164, no. 4, 2023, Art. no. 5242A.

[42] J. Reisenauer, J. Duke, R. Kern, S. Fernandez-Bussy, and E. Edell, "The combination of shape sensing robotic bronchoscopy with mobile 3d imaging to verify tool-in-lesion and assess divergence," *Chest*, vol. 160, no. 4, 2021, Art. no. 2529A.

[43] J. Chambers, D. Knox, and T. Leclair, "O-arm CT for confirmation of successful navigation during robotic assisted bronchoscopy," *J. Bronchol. Int. Pulmonol.*, vol. 30, no. 2, pp. 155–162, 2023.

[44] C. F. Graetzel, A. Sheehy, and D. P. Noonan, "Robotic bronchoscopy drive mode of the auris monarch platform," in *Proc. IEEE Int. Conf. Robot. Autom. (ICRA)*, 2019, pp. 3895–3901.

[45] M. J. Diddams and H. J. Lee, "Robotic bronchoscopy: Review of three systems," *Life*, vol. 13, no. 2, p. 354, 2023.

[46] J. Lin and D. E. Ost, "Robotic bronchoscopy for peripheral pulmonary lesions: A convergence of technologies," *Current Opin. Pulmonary Med.*, vol. 27, no. 4, pp. 229–239, 2021.

[47] F. Xie, A. Wagh, R. Wu, D. K. Hogarth, and J. Sun, "Robotic-assisted bronchoscopy in the diagnosis of peripheral pulmonary lesions," *Chin. Med. J. Pulmonary Crit. Care Med.*, vol. 1, no. 1, pp. 30–35, 2023.

[48] G. Ortiz-Jaimes and J. Reisenauer, "Real-world impact of robotic-assisted bronchoscopy on the staging and diagnosis of lung cancer: The shape of current and potential opportunities," *Pragmatic Observational Res.*, vol. 14, pp. 75–94, Sep. 2023.

[49] N. Ravikumar, E. Ho, A. Wagh, and S. Murgu, "Advanced imaging for robotic bronchoscopy: A review," *Diagnostics*, vol. 13, no. 5, p. 990, 2023.

[50] S. V. Kemp, "Navigation bronchoscopy," *Respiration*, vol. 99, no. 4, pp. 277–286, 2020.

[51] R. M. G. Prado, J. Cicenia, and F. A. Almeida, "Robotic-assisted bronchoscopy: A comprehensive review of system functions and analysis of outcome data," *Diagnostics*, vol. 14, no. 4, p. 399, 2024.

[52] A. Agrawal, D. K. Hogarth, and S. Murgu, "Robotic bronchoscopy for pulmonary lesions: A review of existing technologies and clinical data," *J. Thoracic Disease*, vol. 12, no. 6, pp. 3279–3286, 2020.

[53] A. Talon, S. Chundu, M. Wang, M. Javed, A. I. Khokar, and A. I. Saeed, "Adjunctive use of disposable 1.1-mm cryoprobe with robotic-assisted bronchoscopy," *Chest*, vol. 162, no. 4, 2022, Art. no. 2072A.

[54] K. Nishiyama et al., "Clinical utility of rapid on-site evaluation of brush cytology during bronchoscopy using endobronchial ultrasound with a guide sheath," *Sci. Rep.*, vol. 14, no. 1, 2024, Art. no. 21334.

[55] H. De Leon et al., "Device safety assessment of bronchoscopic microwave ablation of normal swine peripheral lung using robotic-assisted bronchoscopy," *Int. J. Hyperthermia*, vol. 40, no. 1, 2023, Art. no. 2187743.

[56] C.-H. Zhong et al., "Feasibility and safety of radiofrequency ablation guided by bronchoscopic transparenchymal nodule access in canines," *Respiration*, vol. 100, no. 11, pp. 1097–1104, 2021.

[57] A. D. Lerner and D. Feller-Kopman, "Is bronchoscopic treatment of lung cancer possible?" *Exp. Rev. Res. Med.*, vol. 13, no. 1, pp. 1–3, 2018.

[58] R. V. Patel, S. F. Atashzar, and M. Tavakoli, "Haptic feedback and force-based teleoperation in surgical robotics," *Proc. IEEE*, vol. 110, no. 7, pp. 1012–1027, Jul. 2022.

[59] J. Reisenauer et al., "Ion: Technology and techniques for shape-sensing robotic-assisted bronchoscopy," *Ann. Thoracic Surg.*, vol. 113, no. 1, pp. 308–315, 2022.

[60] P. E. Dupont, N. Simaan, H. Choset, and C. Rucker, "Continuum robots for medical interventions," *Proc. IEEE*, vol. 110, no. 7, pp. 847–870, Jul. 2022.

[61] K.-W. Kwok, H. Wurdemann, A. Arezzo, A. Menciassi, and K. Althoefer, "Soft robot-assisted minimally invasive surgery and interventions: Advances and outlook," *Proc. IEEE*, vol. 110, no. 7, pp. 871–892, Jul. 2022.

[62] C. Shi et al., "Shape sensing techniques for continuum robots in minimally invasive surgery: A survey," *IEEE Trans. Biomed. Eng.*, vol. 64, no. 8, pp. 1665–1678, Aug. 2017.

[63] A. C. Koumbourlis, *Flexible Bronchoscopy Training*. Cham, Switzerland: Springer Int., 2021, pp. 171–185.

[64] M. McCandless, A. Perry, N. DiFilippo, A. Carroll, E. Billatos, and S. Russo, "A soft robot for peripheral lung cancer diagnosis and therapy," *Soft Robot.*, vol. 9, no. 4, pp. 754–766, 2022.

[65] F. Asano, "Advanced bronchoscopy for the diagnosis of peripheral pulmonary lesions," *Resp. Invest.*, vol. 54, no. 4, pp. 224–229, 2016.

[66] N. Liu, M. E. M. K. Abdelaziz, M. Shen, and G.-Z. Yang, "Design and kinematics characterization of a laser-profiled continuum manipulator for the guidance of bronchoscopic instruments," in *Proc. IEEE Int. Conf. Robot. Autom. (ICRA)*, 2018, pp. 25–31.

[67] Y. Duan, J. Ling, Z. Feng, T. Ye, T. Sun, and Y. Zhu, "A survey of needle steering approaches in minimally invasive surgery," *Ann. Biomed. Eng.*, vol. 52, no. 6, pp. 1492–1517, 2024.

[68] J. G. Karstensen and P. Vilmann, "Historical perspective on needle development: From the past to the future," *Pract. Res. Clin. Gastroenterol.*, vols. 60–61, Sep./Oct. 2022, Art. no. 101814.

[69] J. Zhang, Q. Fang, P. Xiang, R. Xiong, Y. Wang, and H. Lu, "Soft hybrid actuated hierarchical bronchoscope robot for deep lung examination," *IEEE Robot. Autom. Lett.*, vol. 9, no. 1, pp. 811–818, Jan. 2024.

[70] G. Pittiglio et al., "Personalized magnetic tentacles for targeted photothermal cancer therapy in peripheral lungs," *Commun. Eng.*, vol. 2, no. 1, p. 50, 2023.

[71] T. Goto, "Robotic bronchoscopy: Is it classic?" *J. Thoracic Disease*, vol. 13, no. 1, pp. 409–410, 2021.

[72] O. B. Rickman, A. K. Mahajan, D. K. Hogarth, and K. Bhadra, "'Tool-in-lesion' accuracy of galaxy system: Robotic-assisted, electromagnetic navigation bronchoscopy with integrated tool-in-lesion-tomosynthesis technology: The match study," *Chest*, vol. 162, no. 4, pp. 2650–2651, 2022.

[73] F. Diaz-Churion et al., "Real-time visualization of lung malignancy with needle-based confocal laser endomicroscopy during shape-sensing robotic-assisted bronchoscopy," *Respirol. Case Rep.*, vol. 11, no. 3, 2023, Art. no. e01092.

[74] F. J. Herth, S. Li, J. Sun, B. Lam, D. Nader, and J. Idris, "Bronchoscopic biopsy of solitary pulmonary nodules with no leading airway path," *Eur. Resp. J.*, vol. 52, no. S62, 2018, Art. no. OA2167.

[75] A. Kuntz et al., "Autonomous medical needle steering in vivo," *Sci. Robot.*, vol. 8, no. 82, 2023, Art. no. eadf7614.

[76] A. Donder and F. R. Y. Baena, "3-D path-following control for steerable needles with fiber Bragg gratings in multi-core fibers," *IEEE Trans. Biomed. Eng.*, vol. 70, no. 3, pp. 1072–1085, Mar. 2023.

[77] R. L. Pratt and A. J. Petruska, "Magnetic needle steering control using Lyapunov redesign," *Int. J. Robot. Res.*, vol. 43, no. 11, p. 1449, 2024.

[78] A. Gao et al., "Laser-profiled continuum robot with integrated tension sensing for simultaneous shape and tip force estimation," *Soft Robot.*, vol. 7, no. 4, pp. 421–443, 2020.

[79] X. Ai, A. Gao, Z. Lin, C. He, and W. Chen, "A multi-contact-aided continuum manipulator with anisotropic shapes," *IEEE Robot. Autom. Lett.*, vol. 6, no. 3, pp. 4560–4567, Jul. 2021.

[80] G.-B. Bian et al., "Design and nonlinear error compensation of a multi-segment soft continuum robot for pulmonary intervention," *IEEE Trans. Med. Robot. Bionics*, vol. 5, no. 4, pp. 832–842, Nov. 2023.

[81] X. Duan et al., "A novel robotic bronchoscope system for navigation and biopsy of pulmonary lesions," *Cyborg Bionic Syst.*, vol. 4, p. 13, Mar. 2023.

[82] X. Ai, Y. Cai, A. Gao, and W. Chen, "A steerable cross-axis notched continuum manipulator for endobronchial intervention," *IEEE Trans. Med. Robot. Bionics*, vol. 6, no. 2, pp. 498–511, May 2024.

[83] Y. Li, J. Peine, M. Mencattelli, J. Wang, J. Ha, and P. E. Dupont, "A soft robotic balloon endoscope for airway procedures," *Soft Robot.*, vol. 9, no. 5, pp. 1014–1029, 2022.

[84] D. Van Lewen, T. Janke, H. Lee, R. Austin, E. Billatos, and S. Russo, "A millimeter-scale soft robot for tissue biopsy procedures," *Adv. Intell. Syst.*, vol. 5, no. 5, 2023, Art. no. 2200326.

[85] J. Davy et al., "Vine robots with magnetic skin for surgical navigations," *IEEE Robot. Autom. Lett.*, vol. 9, no. 8, pp. 6888–6895, Aug. 2024.

[86] N. Murasovs et al., "Breathing compensation in magnetic robotic bronchoscopy via shape forming," *IEEE Robot. Autom. Lett.*, vol. 9, no. 10, pp. 9055–9062, Oct. 2024.

[87] T. Zhang et al., "Sub-millimeter fiberscopic robot with integrated maneuvering, imaging, and biomedical operation abilities," *Nat. Commun.*, vol. 15, no. 1, 2024, Art. no. 10874.

[88] P. J. Swaney et al., "Toward transoral peripheral lung access: Combining continuum robots and steerable needles," *J. Med. Robot. Res.*, vol. 2, no. 1, 2017, Art. no. 1750001.

[89] T. Kato, F. King, K. Takagi, and N. Hata, "Robotized catheter with enhanced distal targeting for peripheral pulmonary biopsy," *IEEE/ASME Trans. Mechatronics*, vol. 26, no. 5, pp. 2451–2461, Oct. 2021.

[90] Z. Mitros, B. Thamo, C. Bergeles, L. da Cruz, K. Dhaliwal, and M. Khadem, "Design and modelling of a continuum robot for distal lung sampling in mechanically ventilated patients in critical care," *Front. Robot. AI*, vol. 8, Jun. 2021, Art. no. 611866.

[91] J. Wang, C. Hu, J. Kang, J. Liu, L. Ma, and H. Liao, "A novel robotic bronchoscope with a spring-based extensible segment for improving steering ability," in *Proc. IEEE Int. Conf. Robot. Autom. (ICRA)*, 2024, pp. 15448–15454.

[92] P. Swaney, H. Gilbert, R. Hendrick, O. Commichau, R. Alterovitz, and R. Webster, "Transoral steerable needles in the lung: How non-annular concentric tube robots can improve targeting," in *Proc. Hamlyn Symp. Med. Robot.*, 2015, pp. 37–38.

[93] M. Rox et al., "Decoupling steerability from diameter: Helical dovetail laser patterning for steerable needles," *IEEE Access*, vol. 8, pp. 181411–181419, 2020.

[94] L. Ros-Freixedes, A. Gao, N. Liu, M. Shen, and G.-Z. Yang, "Design optimization of a contact-aided continuum robot for endobronchial interventions based on anatomical constraints," *Int. J. Comput. Assist. Radiol. Surg.*, vol. 14, no. 7, pp. 1137–1146, 2019.

[95] X. Ai, A. Gao, and W. Chen, "Anatomy-specific optimization of a multi-contact-aided continuum manipulator," *IEEE Trans. Med. Robot. Bionics*, vol. 6, no. 1, pp. 84–95, Feb. 2024.

[96] S. Yuan et al., "Motor-free telerobotic endomicroscopy for steerable and programmable imaging in complex curved and localized areas," *Nat. Commun.*, vol. 15, no. 1, p. 7680, 2024.

[97] B. J. Nelson, S. Gervasoni, P. W. Y. Chiu, L. Zhang, and A. Zemmar, "Magnetically actuated medical robots: An in vivo perspective," *Proc. IEEE*, vol. 110, no. 7, pp. 1028–1037, Jul. 2022.

[98] Y. Kim, G. A. Parada, S. Liu, and X. Zhao, "Ferromagnetic soft continuum robots," *Sci. Robot.*, vol. 4, no. 33, 2019, Art. no. eaax7329.

[99] C. He et al., "Magnetically actuated dexterous tools for minimally invasive operation inside the brain," *Sci. Robot.*, vol. 10, no. 100, 2025, Art. no. eadk4249.
[100] Y. Kim and X. Zhao, "Magnetic soft materials and robots," *Chem. Rev.*, vol. 122, no. 5, pp. 5317–5364, 2022.
[101] J. Hu et al., "Magnetic soft catheter robot system for minimally invasive treatments of articular cartilage defects," *Soft Robot.*, vol. 11, no. 6, pp. 1032–1042, 2024.
[102] G. Pittiglio et al., "Patient-specific magnetic catheters for atraumatic autonomous endoscopy," *Soft Robot.*, vol. 9, no. 6, pp. 1120–1133, 2022.
[103] C. Culmone, F. S. Yikilmaz, F. Trauzettel, and P. Breedveld, "Follow-the-leader mechanisms in medical devices: A review on scientific and patent literature," *IEEE Rev. Biomed. Eng.*, vol. 16, pp. 439–455, 2023.
[104] G. Pittiglio, J. H. Chandler, M. Richter, V. K. Venkiteswaran, S. Misra, and P. Valdastri, "Dual-arm control for enhanced magnetic manipulation," in *Proc. IEEE/RSJ Int. Conf. Intell. Robots Syst. (IROS)*, 2020, pp. 7211–7218.
[105] M. Li, A. Pal, A. Aghakhani, A. Pena-Francesch, and M. Sitti, "Soft actuators for real-world applications," *Nat. Rev. Mater.*, vol. 7, pp. 235–249, Nov. 2022.
[106] G. Fang et al., "Soft robotic manipulator for intraoperative MRI-guided transoral laser microsurgery," *Sci. Robot.*, vol. 6, no. 57, 2021, Art. no. eabg5575.
[107] M. McCandless, A. Gerald, A. Carroll, H. Aihara, and S. Russo, "A soft robotic sleeve for safer colonoscopy procedures," *IEEE Robot. Autom. Lett.*, vol. 6, no. 3, pp. 5292–5299, May 2021.
[108] K. Borvorntanajanya, S. Treratanakulchai, F. R. Y. Rodriguez, and E. Franco, "Model-based tracking control of a soft growing robot for colonoscopy," *IEEE Trans. Med. Robot. Bionics*, vol. 6, no. 4, pp. 1354–1362, Mar. 2025.
[109] X.-Y. Chen et al., "Robotic bronchoscopy system with variable-stiffness catheter for pulmonary lesion biopsy," *IEEE Trans. Med. Robot. Bionics*, vol. 7, no. 1, pp. 416–427, Feb. 2025.
[110] C. Baykal, L. G. Torres, and R. Alterovitz, "Optimizing design parameters for sets of concentric tube robots using sampling-based motion planning," in *Proc. IEEE/RSJ Int. Conf. Intell. Robots Syst. (IROS)*, 2015, pp. 4381–4387.
[111] J. Wang, C. Hu, Y. Sun, L. Ma, G. Ning, and H. Liao, "Preliminary study of a spring-based miniature extensible manipulator for bronchoscopic steering," in *Proc. IEEE Int. Conf. Robot. Biomimetics (ROBIO)*, pp. 1–6.
[112] G.-B. Bian et al., "Accurate shape and tip-contact-force estimation of multisegment continuum-robotic tubular bronchoscopes," *IEEE/ASME Trans. Mechatronics*, early access, Jan. 24, 2025, doi: 10.1109/TMECH.2024.3523971.
[113] C. D. Remy, Z. Brei, D. Bruder, J. Remy, K. Buffinton, and R. B. Gillespie, "The 'fluid jacobian': Modeling force-motion relationships in fluid-driven soft robots," *Int. J. Robot. Res.*, vol. 43, no. 5, pp. 628–645, 2024.
[114] I. E. Commission et al. "IEC TR 60601-4-1—Medical electrical equipment–part 4-1: Guidance and interpretation-medical electrical equipment and medical electrical systems employing a degree of autonomy." 2017. [Online]. Available: https://webstore.iec.ch/publicatio
[115] A. Pore et al., "Autonomous navigation for robot-assisted intraluminal and endovascular procedures: A systematic review," *IEEE Trans. Robot.*, vol. 39, no. 4, pp. 2529–2548, Jan. 2023.
[116] J. Sganga, D. Eng, C. Graetzel, and D. B. Camarillo, "Autonomous driving in the lung using deep learning for localization," 2019, *arXiv:1907.08136*.
[117] M. Shen, Y. Gu, N. Liu, and G.-Z. Yang, "Context-aware depth and pose estimation for bronchoscopic navigation," *IEEE Robot. Autom. Lett.*, vol. 4, no. 2, pp. 732–739, Apr. 2019.
[118] C. Zhao, M. Shen, L. Sun, and G.-Z. Yang, "Generative localization with uncertainty estimation through video-CT data for bronchoscopic biopsy," *IEEE Robot. Autom. Lett.*, vol. 5, no. 1, pp. 258–265, Jan. 2020.
[119] A. Banach, F. King, F. Masaki, H. Tsukada, and N. Hata, "Visually navigated bronchoscopy using three cycle-consistent generative adversarial network for depth estimation," *Med. Image Anal.*, vol. 73, Jul. 2021, Art. no. 102164.
[120] Y. Gu, C. Gu, J. Yang, J. Sun, and G. Z. Yang, "Vision-kinematics interaction for robotic-assisted bronchoscopy navigation," *IEEE Trans. Med. Imag.*, vol. 41, no. 12, pp. 3600–3610, Mar. 2022.
[121] Q. Tian et al., "Bronchotrack: Airway lumen tracking for branch-level bronchoscopic localization," *IEEE Trans. Med. Imag.*, vol. 44, no. 3, pp. 1321–1333, Mar. 2025, doi: 10.1109/TMI.2024.3493170.
[122] A. Kuntz, L. G. Torres, R. H. Feins, I. Webster, J. Robert, and R. Alterovitz, "Motion planning for a three-stage multilumen transoral lung access system," in *Proc. IEEE/RSJ Int. Conf. Intell. Robots Syst. (IROS)*, 2015, pp. 3255–3261.
[123] M. Fu, A. Kuntz, I. Webster, J. Robert, and R. Alterovitz, "Safe motion planning for steerable needles using cost maps automatically extracted from pulmonary images," in *Proc. IEEE/RSJ Int. Conf. Intell. Robots Syst. (IROS)*, 2018, pp. 4942–4949.
[124] J. Hoelscher et al., "Backward planning for a multi-stage steerable needle lung robot," *IEEE Robot. Autom. Lett.*, vol. 6, no. 2, pp. 3987–3994, 2021.
[125] M. Fu, K. Solovey, O. Salzman, and R. Alterovitz, "Resolution-optimal motion planning for steerable needles," in *Proc. IEEE Int. Conf. Robot. Autom. (ICRA)*, 2022, pp. 9652–9659.
[126] G.-B. Bian et al., "Few-human-interaction reinforcement learning for autonomous transbronchial intervention," *IEEE Trans. Neural Netw. Learn. Syst.*, early access, Sep. 13, 2024, doi: 10.1109/TNNLS.2024.3452944.
[127] J. Sganga, "Autonomous navigation of a flexible surgical robot in the lungs," *Cureus*, vol. 16, no. 1, Jan. 2024, Art. no. e52243.
[128] Z. Lin et al., "ARei: Augmented-reality-assisted touchless teleoperated robot for endoluminal intervention," *IEEE/ASME Trans. Mechatronics*, vol. 27, no. 5, pp. 3144–3154, Oct. 2022.
[129] Y. Zou, B. Guan, J. Zhao, S. Wang, X. Sun, and J. Li, "Robotic-assisted automatic orientation and insertion for bronchoscopy based on image guidance," *IEEE Trans. Med. Robot. Bionics*, vol. 4, no. 3, pp. 588–598, Aug. 2022.
[130] J. Zhang et al., "Ai co-pilot bronchoscope robot," *Nat. Commun.*, vol. 15, no. 1, p. 241, 2024.
[131] D. Van Lewen et al., "A real-time, semi-autonomous navigation platform for soft robotic bronchoscopy," *IEEE Robot. Autom. Lett.*, vol. 10, no. 5, pp. 4722–4729, May 2025.
[132] W. D. Bolton, H. Howe, and J. E. Stephenson, "The utility of electromagnetic navigational bronchoscopy as a localization tool for robotic resection of small pulmonary nodules," *Ann. Thoracic Surg.*, vol. 98, no. 2, pp. 471–476, 2014.
[133] H. Liu, S. Zhang, Y. Yang, L. Sun, Z. Song, and S. Xu, "A robust pose optimization scheme with spatial geometry awareness for hybrid bronchoscopic navigation," *IEEE Trans. Instrum. Meas.*, vol. 73, pp. 1–10, 2024.
[134] A. Sorriento et al., "Optical and electromagnetic tracking systems for biomedical applications: A critical review on potentialities and limitations," *IEEE Rev. Biomed. Eng.*, vol. 13, pp. 212–232, 2020.
[135] I. Fried, J. Hoelscher, J. A. Akulian, S. Pizer, and R. Alterovitz, "Landmark based bronchoscope localization for needle insertion under respiratory deformation," in *Proc. IEEE/RSJ Int. Conf. Intell. Robots Syst. (IROS)*, 2023, pp. 6593–6600.
[136] X. Luo and K. Mori, "A discriminative structural similarity measure and its application to video-volume registration for endoscope three-dimensional motion tracking," *IEEE Trans. Med. Imag.*, vol. 33, no. 6, pp. 1248–1261, Jun. 2014.
[137] S. A. Merritt, R. Khare, R. Bascom, and W. E. Higgins, "Interactive CT-video registration for the continuous guidance of bronchoscopy," *IEEE Trans. Med. Imag.*, vol. 32, no. 8, pp. 1376–1396, Mar. 2013.
[138] L. Yang, J. Qi, D. Song, J. Xiao, J. Han, and Y. Xia, "Survey of robot 3-D path planning algorithms," *J. Control Sci. Eng.*, vol. 2016, 2016, Art. no. 7426913.
[139] X. Zang et al., "Optimal route planning for image-guided EBUS bronchoscopy," *Comput. Biol. Med.*, vol. 112, Jun. 2019, Art. no. 103361.
[140] L. Karstensen et al., "Learning-based autonomous vascular guidewire navigation without human demonstration in the venous system of a porcine liver," *Int. J. Comput. Assist. Radiol. Surg.*, vol. 17, no. 11, pp. 2033–2040, 2022.
[141] J. Kweon et al., "Deep reinforcement learning for guidewire navigation in coronary artery phantom," *IEEE Access*, vol. 9, pp. 166409–166422, 2021.
[142] A. Pore et al., "Colonoscopy navigation using end-to-end deep visuomotor control: A user study," in *Proc. IEEE/RSJ Int. Conf. Intell. Robots Syst. (IROS)*, 2022, pp. 9582–9588.
[143] J. Sganga, D. Eng, C. Graetzel, and D. Camarillo, "OffsetNet: Deep learning for localization in the lung using rendered images," in *Proc. Int. Conf. Robot. Autom. (ICRA)*, 2020, pp. 5046–5052.
[144] J. Zhao et al., "BronchoCopilot: Towards autonomous robotic bronchoscopy via multimodal reinforcement learning," in *Proc. IEEE/RSJ Int. Conf. Intell. Robots Syst. (IROS)*, 2024, pp. 6923–6930.

[145] Q. Tian et al., "DD-VNB: A depth-based dual-loop framework for real-time visually navigated bronchoscopy," in *Proc. IEEE/RSJ Int. Conf. Intell. Robots Syst. (IROS)*, 2024, pp. 12979–12986.
[146] Z. Lin et al., "Robotic manipulator-assisted omnidirectional augmented reality for endoluminal intervention telepresence," *Adv. Intell. Syst.*, vol. 6, no. 1, 2023, Art. no. 2300373.
[147] D. P. Losey, C. G. McDonald, E. Battaglia, and M. K. O'Malley, "A review of intent detection, arbitration, and communication aspects of shared control for physical human–robot interaction," *Appl. Mech. Rev.*, vol. 70, no. 1, 2018, Art. no. 10804.
[148] J. Zhang et al., "A novel handheld bronchoscope robot with human–robot shared control strategy for pulmonary examination," *IEEE/ASME Trans. Mechatronics*, early access, Oct. 7, 2024, doi: 10.1109/TMECH.2024.3462454.
[149] J. Hoelscher, I. Fried, S. Tsalikis, J. Akulian, R. J. Webster, and R. Alterovitz, "Safe start regions for medical steerable needle automation," *IEEE Trans. Robot.*, vol. 41, pp. 2424–2440, 2025.
[150] M. Selvaggio, M. Cognetti, S. Nikolaidis, S. Ivaldi, and B. Siciliano, "Autonomy in physical human–robot interaction: A brief survey," *IEEE Robot. Autom. Lett.*, vol. 6, no. 4, pp. 7989–7996, Oct. 2021.
[151] A. Sachdeva and J. Singh, "Successful biopsy of aortopulmonary window lymph node with robotic-assisted bronchoscopy," *Chest*, vol. 162, no. 4, 2022, Art. no. A2108.
[152] D. M. Wisa et al., "Accessing aortopulmonary lymph nodes via robotic-assisted bronchoscopy: A new 'window' of opportunity," *Chest*, vol. 164, no. 4, pp. A5238–A5239, 2023.
[153] K. Howk, W. Dickhans, K. Rooks, F. D. M. Nonalaya, and K. Haley, *Characterization of a Bronchoscopic Thermal Ablation Catheter in Porcine Lung*, Amer. Thoracic Soc., New York, NY, USA, 2016, pp. A6019–A6019.
[154] T. Koizumi et al., "Bronchoscopy-guided cooled radiofrequency ablation as a novel intervention therapy for peripheral lung cancer," *Respiration*, vol. 90, no. 1, pp. 47–55, 2015.
[155] X. Yang et al., "Application of 5G technology to conduct tele-surgical robot-assisted laparoscopic radical cystectomy," *Int. J. Med. Robot. Compu. Assist. Surgery*, vol. 18, no. 4, 2022, Art. no. e2412.